

Automotive catalyst warm-up to light-off by pulsating engine exhaust

Benjamin, S.F. and Roberts, C.A.

Author post-print (accepted) deposited in CURVE June 2013

Original citation & hyperlink:

Benjamin, S.F. and Roberts, C.A. (2004) Automotive catalyst warm-up to light-off by pulsating engine exhaust. International Journal of Engine Research, volume 5 (2): 125-147
<http://dx.doi.org/10.1243/146808704773564541>

Copyright © and Moral Rights are retained by the author(s) and/ or other copyright owners. A copy can be downloaded for personal non-commercial research or study, without prior permission or charge. This item cannot be reproduced or quoted extensively from without first obtaining permission in writing from the copyright holder(s). The content must not be changed in any way or sold commercially in any format or medium without the formal permission of the copyright holders.

This document is the author's post-print version of the journal article, incorporating any revisions agreed during the peer-review process. Some differences between the published version and this version may remain and you are advised to consult the published version if you wish to cite from it.

CURVE is the Institutional Repository for Coventry University

<http://curve.coventry.ac.uk/open>

AUTOMOTIVE CATALYST WARM UP TO LIGHT-OFF BY PULSATING ENGINE EXHAUST

S. F. Benjamin and C. A. Roberts

School of Engineering, Coventry University, CV1 5FB, UK

ABSTRACT

This paper presents the results of studies on a range of different catalyst substrates warmed by engine exhaust. Engine speeds were in the range 1200 to 3000 rpm. One substrate was non-washcoated, four were washcoated but non-reactive, and four were washcoated and reactive. The temperature at four locations within the non-reactive substrates was measured. The reactive substrates were warmed to light off by the pulsating exhaust flow from an engine running fuel rich of stoichiometric. Both substrate temperatures and hydrocarbon conversion were measured. Predicted temperatures and conversion were obtained from a 1D CFD model. The model was based on the porous medium approach and incorporated a simple 3-way chemical scheme. Comparison was made of measurements with predictions, with particular reference to the time taken to achieve light-off. Pulsing flow CFD predictions were found to be almost identical to steady flow predictions for the conditions investigated. The CFD predictions were found to be in fair agreement with the engine test results, but using kinetic rate constants higher than previously reported values.

KEY WORDS: automotive catalyst, light-off, pulsating flow, substrate temperature, hydrocarbon conversion

NOTATION

| | |
|----------|---|
| A | channel cross sectional area |
| A_v | wetted surface area per unit volume of catalyst substrate |
| C_i | concentration of species, mass per unit volume |
| C_o | concentration at inlet |
| C_z | concentration at z |
| C_{si} | concentration of species i at reactive surface |
| C_{gi} | concentration of species i in exhaust gas |

| | |
|------------------|--|
| C_{pg} | thermal capacity of exhaust gas |
| C_w | thermal capacity of substrate wall material |
| [CO] | mass fraction of species CO |
| d_h | hydraulic diameter of channel |
| D_m | mass diffusivity |
| E_i | activation energy |
| Fi | mass flow of species i |
| h | heat transfer coefficient |
| ΔH_i | heat of reaction for species i |
| k_{o1}, k_{o2} | reaction rate constants, expressed in mol/s/m ³ |
| k_1, k_2, k_3 | reaction rate constants, expressed in mol/K/s/m ² noble metal |
| k_g | thermal conductivity of exhaust gas |
| k_s | thermal conductivity of solid substrate |
| K_{mi} | mass transfer coefficient for species i |
| m | instantaneous mass flow rate |
| M | arbitrary multiplier |
| Mi | molar mass of species i, in kg/mol |
| P | channel perimeter |
| Nu | Nusselt number ($h d_h / k_g$) |
| Ri | reaction rate for consumption of species i, mol/s/m ³ |
| R | gas constant |
| t | time |
| S | mass transport source term |
| Se | additional enthalpy source term for chemical reactions |
| Sh | Sherwood number ($h_m d_h / D_m$) |
| T | time period of mass flow pulsations |
| T_g | exhaust gas temperature |
| T_w | solid substrate or channel wall temperature |
| U, V, W | velocity components |
| U_c | channel velocity |

| | |
|---------------|------------------------------------|
| x,y,z | Cartesian coordinates |
| ε | porosity fraction |
| ρ_s | density of substrate wall material |
| ρ_g | density of exhaust gas |

1.0 INTRODUCTION

This paper concerns the warm up to light off of automotive catalyst substrates by pulsating engine exhaust. Warm up to light off temperature is important because until the catalyst becomes active at the light off temperature, unconverted pollutants are expelled in the exhaust to the atmosphere. Testing of catalysts on engine test beds is an expensive and time-consuming procedure. A technique is needed for prediction of light off of a substrate under the flow conditions that are experienced in an exhaust system. Prediction techniques require a model that can predict the warm up of the substrate prior to light off and can additionally account for the effects of the chemical processes that occur as light off is initiated. The simplest chemical schemes consider only oxidation of CO and hydrocarbons, the latter being usually represented by propene, C_3H_6 . Such models can realistically describe the processes in the exhaust of lean burn (fuel lean) engines with simple Pt catalysts.

Models of this type were first developed almost twenty years ago [1] and were amenable to numerical solution processes [2]. Tagliaferri et al. [3] simplified the kinetics of a complex mixture of gases by considering the oxidation of an equivalent amount of CO. They investigated lambda cycling and intermittent, rather than pulsing, flow. Recently many of the models reported in the literature have been extended to include three-way catalysis whereby more complex mixtures of Pt/Pd and Rh enabled reduction of NO simultaneously with the oxidation of other species. The work of Siemund et al. [4] exemplifies this approach. They compared predictions with a limited amount of measured data on temperature and conversion obtained from engine tests. Other workers have added greater complexity to the chemical scheme by including the oxidation of slow and fast hydrocarbons and oxidation of hydrogen, for example the work by Koltsakis et al., [5]. The latter have published very widely on this topic and this particular reference is a recent and representative example of their approach. Their 1998 paper reports a two-dimensional model and also includes an oxygen storage submodel. Computed and measured data for lambda excursions are presented. Other workers have also considered oxygen

storage in engine excursions between fuel rich and fuel lean (for example Pattas et al., [6] and Schweich, [7]). Recently Baba et al. [8] have tried to look at deactivation of the catalyst by ageing mechanisms as well as the influence of oxygen storage. There are other reactions that are known to occur in automotive catalysts, for example steam reforming, included in [5], and some which are not yet generally included, for example water gas shift. Models must, however, strike a balance between a complete chemical description and one that is computationally efficient and which will provide useful predictions in an industrial context. Many of the models described in the literature are 1D and non-pulsating. Any attempt to fully model 2D geometries, for example McCullough et al., [9] introduces flow field and thermal problems, which add unnecessary complexity for validating the reaction modelling. A recent 1D modelling exercise reported by Lacin and Zhuang [10] included pulsating flow. Their inlet temperature was constant at 600K, which is above the expected light-off temperature. They found, as would be expected, that a pulsating mass flow causes the degree of conversion at exit to vary periodically. Conversion pulsations are out of phase with mass flow pulsations, because conversion is higher for lower mass flow rates.

The present authors have considered 1D warm up under pulsating flow conditions [11]. Work on an experimental test rig under non reacting conditions showed a very small effect of approximately sinusoidal pulsations in mass flow rate on warm up. This work has been extended to less idealised conditions on an engine test bed with non-sinusoidal pulsating flow and the data obtained are presented in this paper.

The literature on this subject is extensive, but the majority of the work is simulation based, although with some containing limited experimental data. The work reported here, however, covers both measurements and CFD predictions and in particular examines the onset of light off under pulsating flow conditions. These were well-controlled engine tests with measurements being made of both temperature and hydrocarbon conversion. In the tests the temperature was ramped up at about 5K/s as would be the case in a practical warming under floor catalyst. The temperatures were measured to provide a thermal map of temperature distribution within the substrate, rather than solely gas temperatures at inlet and exit. The tests were performed on both non-reactive and reactive substrates and were designed to look at a range of substrate properties. Nine different substrate types and three

engine speeds were investigated. Warm up of the non-reactive substrates by the pulsating engine exhaust provided data for looking at the ability of the model to predict temperature.

The commercial CFD package Star-CD was used for this work. The porous medium approach [12] can model fully the flow distribution, heat and mass transfer and chemical reactions in a 2D or 3D case without any need for detailed single channel modelling. The rationale in using CFD at this stage on what is essentially a 1D study is so that the model, once developed, can be directly applied to full 3D flow cases in future work.

The CFD model uses a simple three-way chemical model to make 1D predictions of temperature and conversion. The time taken to achieve light-off is of particular interest since this determines the effectiveness of a particular substrate in reducing emissions. It is an important criterion against which the performance of the model can be assessed. The porous medium model was originally developed for predicting temperatures prior to light off [12]. The ability of the model to predict light-off is dependent upon its ability to predict temperature prior to light-off. Measurements of warm up of the reactive substrates provided data for testing the ability of the model in predicting light-off. This work is thus a systematic and thorough test of the predictions made by the model over a wide range of conditions. There is particular emphasis on the ability of the model to predict the onset of light-off when the mass flow is pulsating, as in real exhaust systems.

2.0 THEORY

2.1 Basis of CFD model

The heat transfer occurring during warm up prior to light off is described by two simultaneous equations, in the gas and in the solid. The co-ordinate system has the substrate axis and flow in the +z direction. The conduction equation for the substrate wall in an isotropic continuum is,

$$\rho_s (1-\varepsilon) C_w \frac{\partial T_w}{\partial t} - (1-\varepsilon) k_s \frac{\partial^2 T_w}{\partial z^2} = -h A_v (T_w - T_g) \quad (1)$$

The energy equation describing the gas is

$$\rho_g \varepsilon C_{pg} \left[\frac{\partial T_g}{\partial t} + W \frac{\partial T_g}{\partial z} \right] - \varepsilon k_g \frac{\partial^2 T_g}{\partial z^2} = -h A_v (T_g - T_w) \quad (2)$$

In (2) it is assumed that turbulent transport of enthalpy is negligible as the unidirectional flow through the catalyst channels is laminar. The quantity A_v (m^2/m^3) is the effective bulk value of wetted area available in the substrate, a value which is specified by manufacturers for their substrate materials, and which is dependent upon whether the surface is washcoated or non washcoated. When the equations are solved numerically, the heat transfer between gas and wall is dealt with as a source term calculated from known heat transfer coefficients.

For reactive catalysts, the model considers three chemical species: CO, C_3H_6 and NO. Oxidation of CO and C_3H_6 and reduction of NO by CO generate no significant products in this simple chemical scheme and so the species are treated as passive scalars. Oxygen is also included as the fourth species. The assumption is made that no reactions occur in the gaseous phase, only at the solid surface. The exothermic reactions contribute an additional source term to the solid phase energy equation (1) above, as discussed below.

The simplified conservation equation for chemical species in the gaseous phase in the exhaust may be expressed, with diffusion neglected, as

$$\frac{\partial}{\partial t} (\rho_g C_{gi}) + \frac{\partial}{\partial x} (\rho_g U C_{gi}) = S \quad (3)$$

Diffusion is assumed to have negligible influence because the flow is laminar through the channels and convective transport dominates the transfer of species. The source term S describes transfer of species from solid to gas.

$$S = -\rho_g K_{mi} A_v (C_{gi} - C_{si}) \quad (4)$$

Since concentration C_{si} will be less than concentration C_{gi} the term S will be a species sink term for the gas cells in the model. Values for mass transfer coefficients K_{mi} and for A_v must be specified. The values for K_{mi} are dependent upon diffusion coefficient values. K_m values used were: 0.2684 m/s for CO, 0.292 m/s for NO, 0.1506 m/s for C_3H_6 and 0.28 m/s for NO.

It is assumed that there is no accumulation of species in the solid phase so the concentration of species on the monolith surface is governed by

$$\rho_g K_{mi} A_v (C_{gi} - C_{si}) = M_i R_i \quad (5)$$

where M_i is molar mass in kg/mol and R_i is reaction rate in the solid phase in mol/sec/m³.

When catalytic reactions occur the temperature equation describing the solid (1) has an extra source term due to the heat released through the chemical oxidation and reduction reactions in the solid phase.

$$S_e = R_i \Delta H_i \quad (6)$$

2.1.1 Oxidation chemistry

The following oxidation reactions are modelled.



The oxidation of carbon monoxide together with propene is taken to represent the more complex reactions that occur in exhaust, which is a mixture of a wider range of species. In the case of fuel lean engine combustion only oxidation need be considered, but for stoichiometric or fuel rich tests reduction of NO is additionally included. This paper does not attempt to determine the reaction rate constants for these reactions, but utilises data available in the open literature. Therefore a brief review follows.

The intrinsic reaction rate constants for CO and C₃H₆ oxidation are the velocity constants k_1 and k_2 respectively. The kinetic scheme is derived from the work of Voltz et al. [13] for a Pt catalyst over a limited temperature range 400 to 700 °F, i.e. 477 to 644 K. In this paper the authors commented that mass transfer becomes the rate controlling mechanism at temperatures above 700 °F (644 K) where intrinsic chemical reaction rates are very fast. Voltz et al. specified values k_{o1} and k_{o2} in imperial units for catalysis by Pt. Converting the original values directly to metric units gives the values:

$$k_{o1} = 6.46\text{E}+17 \exp(-12556/T_s) \quad [\text{mol s}^{-1} \text{ m}^{-3}]$$

$$k_{o2} = 1.34\text{E}+19 \exp(-14556/T_s) \quad [\text{mol s}^{-1} \text{ m}^{-3}]$$

In the paper it is not clear what value was assigned to reactive noble metal surface area per unit volume of reactor, at least not in a way that makes for meaningful comparison with the way the scheme has been used by subsequent authors. The latter have generally used monolithic catalysts rather than pellets. Although subsequent authors have used various values for the reaction rate constants, they have generally retained the original values of Voltz et al., [13] for the adsorption constants. The values

are given below. The term Z_1 is for CO, Z_2 for C₃H₆, Z_3 for the combined effect of CO and C₃H₆ and Z_4 for NO.

$$Z_1 = 65.5 \exp(961/T) \quad (7)$$

$$Z_2 = 2080 \exp(361/T) \quad (8)$$

$$Z_3 = 3.98 \exp(11611/T) \quad (9)$$

$$Z_4 = 4.79E+05 \exp(-3733/T) \quad (10)$$

$$J_1 = (1 + Z_1 C_{CO} + Z_2 C_{C_3H_6})^2 \quad (11)$$

$$J_2 = (1 + Z_3 C_{CO}^2 C_{C_3H_6}^2) \quad (12)$$

$$J_3 = (1 + Z_4 C_{NO}^{0.7}) \quad (13)$$

The functions of the terms J_1 , J_2 and J_3 in the denominator of the reaction rate expression are discussed in the paper by Voltz et al. [13]. The terms J_1 and J_3 are inhibitors that reduce the reaction rate due to the chemisorption of CO and C₃H₆ and to the adsorption for NO respectively. Term J_2 improves the fit to experimental data at higher concentrations of CO and C₃H₆.

$$G_o = J_1 J_2 J_3 \quad (14)$$

$$R_{CO(ox)} = k_{o1} C_{CO} C_{O_2} / G_o \quad [\text{mol s}^{-1} \text{ m}^{-3}]$$

$$R_{C_3H_6} = k_{o2} C_{C_3H_6} C_{O_2} / G_o \quad [\text{mol s}^{-1} \text{ m}^{-3}]$$

The values from the Voltz et al. scheme were re-presented by Oh and Cavendish [1] as

$$k_1 = k_{CO} \exp(-E_{CO}/RT_s) \quad [\text{mol K s}^{-1} \text{ m}^{-2} \text{ Pt}]$$

$$k_2 = k_{HC} \exp(-E_{HC}/RT_s) \quad [\text{mol K s}^{-1} \text{ m}^{-2} \text{ Pt}]$$

where T_s is absolute temperature (K) of the reactive surface. The reaction rate expressions are given below. The concentrations C_{CO} and $C_{C_3H_6}$ are mol fractions of reactants in the vicinity of the noble metal surface. Oh and Cavendish [1] define the denominator G and reaction rates as follows

$$G = J_1 J_2 J_3 T_s \quad (15)$$

$$R_{CO(ox)} = A_{Pt} k_1 C_{CO} C_{O_2} / G \quad [\text{mol s}^{-1} \text{ m}^{-3}]$$

$$R_{C_3H_6} = A_{Pt} k_2 C_{C_3H_6} C_{O_2} / G \quad [\text{mol s}^{-1} \text{ m}^{-3}]$$

$$R_{O_2} = 4.5 R_{C_3H_6} + 0.5 R_{CO(ox)} \quad [\text{mol s}^{-1} \text{ m}^{-3}]$$

The pre- exponential numbers and the activation energies associated with each reaction rate constant have been attributed various values by various authors. Chen and Cole [14] indicated that the chemical kinetics of binary and tertiary catalysts are different from a Pt catalyst. They also discussed the fact that the activation energy has the dominant influence on transient light off. Following from this, Cundari and Nuti [15] have modified the constants to provide values below for a binary Pt/Rh catalyst. Some values from the literature are tabulated in Table 1.

The values for k_1 and k_2 require multiplication by a numerical value for the reactive surface area per unit volume (m^2 noble metal/ m^3 reactor) and division by temperature (K) in order to quantify the reaction rates. The overall reaction rate determined from this scheme is the intrinsic chemical reaction rate, i.e. the effectiveness factor is taken to be unity; the rate calculated from these expressions does not therefore include any effects of species transfer by diffusion within the washcoat layer.

Figure 1 shows values from the literature for the reaction rate constants. The original Voltz et al. values for k_{o1} and k_{o2} given on the previous page have been converted to enable comparison with the k_1 and k_2 values listed above by assuming $4\text{E}+04 \text{ m}^2/\text{m}^3$, temperature 477K, and multiplying by T/A_c . The values of Chan et al. are low, but these authors [16] like others do not specify a numerical value for catalytic surface area per unit catalyst volume, although alignment of values is implicit. The Cundari and Nuti values [15] can be seen to be the only set that significantly alters the way that the reaction rate constant varies with temperature. This scheme was selected for use later because it was appropriate for Pt/Rh binary catalysts on engines, fuel rich exhaust conditions and it provided the best predictions for the shape of the light off curves as observed in the experiments.

2.1.2 Reduction chemistry

The reduction of NO by CO on Rhodium is included in the model.



The reaction rate for this reaction [4] is found as follows

$$k_3 = 3.067\text{E}+12 \exp (-8771/T)$$

$$Z_5 = 1.2028E+05 \exp (653.3/T)$$

$$R_{NO} = R_{CO (red)} = \frac{A_{Rh} k_3 C_{CO}^{1.4} C_{O_2}^{0.3} C_{NO}^{0.13}}{T^{-0.17} (T + Z_5 C_{CO})^2} \quad [\text{mol m}^{-3} \text{s}^{-1}]$$

The concentrations C_i of the various reactants are expressed in mol fractions in the vicinity of the noble metal surface. When this reaction is included the total rate of CO consumption changes to

$$R_{CO} = R_{CO(ox)} + R_{CO(red)} \quad [\text{mol m}^{-3} \text{s}^{-1}]$$

2.2 Methodology for CFD simulations

The mesh was a line of single cells based on the porous medium approach. Four cells represented the inlet, sixty cells represented the 120 mm length of the channels in the porous medium with a further 4 cells representing the fluid at exit. A further sixty cells represented the solid. The measured inlet temperature ramp and mass flow rate from the engine provided the input. Table 2 shows parameter values for the substrates. The initial temperature was near 400K but the value for each experiment was input to the model. The mass fraction of each species at inlet was also input. The resistance of the porous medium to flow was described by the expression below, with α and β permeability values as given in Table 2.

$$\frac{\Delta P}{L} = -\alpha U^2 - \beta U \quad (16)$$

The value for the wetted surface area A_v (m^2/m^3 substrate) was based on the geometry of the substrate channels and was used for calculating heat transfer between fluid and substrate. The washcoat loading was 153 kg of washcoat per m^3 of substrate. It was necessary to consider only axial thermal conductivity of the porous medium in 1D simulations.

The equations were solved using the commercial CFD package Star-CD. The time step for steady flow thermally transient simulations was 0.0015625 secs. The cell length was 2mm and so the time step easily satisfied the criterion that it should be $\ll 50 (L/V)$.

The target area of precious metal A_{PM} m^2/m^3 substrate was estimated from the known loading of the precious metal. The values used in the simulations for the conditioned catalysts were:

$$A_{Pt} \quad 27.0E+04 \quad \text{m}^2/\text{m}^3 \text{ substrate}$$

$$A_{Rh} \quad 9.0E+04 \quad \text{m}^2/\text{m}^3 \text{ substrate}$$

When using Cundari and Nuti [15] values for k_1 and k_2 , the reaction rate constants, an arbitrary multiplier M with value 5 was additionally necessary in order to predict the degree of reactivity observed. If this is considered as an increase in the target area of noble metal surface, the values are too large to be physically realistic. The factor of 5 is thus interpreted as an adjustment to the pre-exponential frequency factor in the reaction rate constant.

2.3 Preliminary parametric studies using CFD model

The performance of the 1D reactive model was explored in a series of parametric studies prior to its evaluation against the engine test data. The effect of mass flow rate on conversion was investigated and the results are shown in Figure 2. These studies considered a 70 mm length substrate with a rising inlet temperature ramp of 5 K/s. The kinetic scheme of Oh and Cavendish, based on Voltz et al., was used, with A_c as $27.0E+04 \text{ m}^2/\text{m}^3$ and an additional arbitrary multiplier of either 1 or 5. The runs were for fuel lean conditions and a range of flow rates equivalent to 4 to 30 g/s to a 50 mm diameter substrate. The arbitrary multiplier affects the reaction rate constant and this modifies the predictions. The mass flow rate has a relatively small effect on predicted light off time. Very high mass flow rates are, however, predicted to pass through the short substrate without being fully converted, even after light off.

After light off, conversion is mass transfer limited, and the fact that predicted conversion is not complete at later times in Fig. 2 is consistent with the following simple analysis. The mass flow of species i

$$F_i = C_i A U_c \quad (17)$$

$$\frac{dC_i}{dz} = - \frac{h_m P C_i}{A U_c} = - \frac{4 C_i h_m}{d_h U_c} = - \frac{4 \text{Sh} D_m C_i}{d_h^2 U_c} \quad (18)$$

$$C_z = C_o \exp -4 \text{Sh} D_m z / (U_c d_h^2) \quad (19)$$

Thus C_z / C_o after light off depends upon $z / (U_c d_h^2)$ and for a certain length of channel z there is a fixed degree of conversion possible dependent upon velocity U_c , as illustrated in Figure 2.

The effect of mass flow pulsations on conversion of CO and hydrocarbons (HC) in a high flow rate case, equivalent to 30 g/s to a 50 mm diameter catalyst, with inlet temperature rising at 5 K/s can be seen in Figure 3. The tube was short, 70 mm, and full conversion was not achieved at this flow rate even after light off. The difference in light off time predicted for steady flow and sinusoidal pulsating flow of amplitude 26 g/s is seen to be very small. There is, however, a small reduction in conversion efficiency when the flow is pulsating. The species conversion fractions in the pulsing cases are mass flow weighted cycle averaged (MWCA). This is defined below, for CO as an example, where Δt is the time step for the numerical computation.

$$\text{Net flow of CO through one cycle} = \sum_0^T \{ m[CO] \Delta t \} \quad (20)$$

$$\text{Flow of gas through one cycle} = \sum_0^T \{ m \Delta t \} \quad (21)$$

$$\text{Mass fraction of CO (MWCA)} = \frac{\sum_0^T \{ m[CO] \}}{\sum_0^T \{ m \}} \quad (22)$$

In the case described as ‘flow and HC pulsing’ in Figure 3 the mass fraction of hydrocarbon at inlet was also pulsing sinusoidally at the same frequency as the mass flow. This further reduces the conversion fraction below the steady flow case but the effect on light-off time is again quite small.

Figure 4 shows the effect of mass flow pulsations in a lower flow rate case, equivalent to 10 g/s to a 50 mm diameter catalyst. The concentration at exit through a cycle of pulsation is shown at 8 distinct times between 15 and 27.5 seconds during the light off process. The normal light off criterion of 50% conversion is achieved on a cycle-averaged basis at about 23 seconds in this case. It can be seen that there is a period of time after 23 seconds when the conversion is total at the low flow parts of the cycle but only 50 % at the high flow parts of the cycle. This breakthrough effect may be significant in close-coupled catalysts that are subjected to a wide range of flow rates during an engine cycle.

This paper now describes the test of this model against experimental data from the engine tests. The engine in the tests was run in an exceptional manner to provide validation data for the model; hence the light off times reported in this paper are not representative of those seen on a production engine.

3.0 METHOD

The catalyst samples were 120 mm in length and 101.6 mm in diameter so that the volume was 0.973 litres. Each sample was drilled with four holes for 0.5 mm thermocouples. The ceramic samples were drilled conventionally whereas the metallic samples were laser drilled. The thermocouples were inserted laterally so that the tips were within 5 mm of the axis of the substrate. The thermocouples were positioned along the z-axis 35, 50, 70 and 85 mm from the inlet face. The substrate washcoat loading was $2.4 \pm 0.15 \text{ g/in}^3$ (153 kg/m^3 approx.).

3.1 Engine test measurement procedure

The exhaust from one bank of a Jaguar V8 engine was supplied through the test section. The pipework between the engine and the test section was lagged. A low angle, slow expansion, conical diffuser upstream of the catalyst provided uniform flow to the substrate. The K type thermocouples probed the samples and Combustion Fast FIDs (Flame Ionisation Detectors) were positioned to sample the hydrocarbons immediately upstream and downstream of the catalyst. These detectors have a response time of 4 ms, which is a substantial improvement over conventional gas analysers. Other chemical species were monitored at exit from the engine. A schematic diagram of the rig is seen in Figure 5.

The fresh catalyst was conditioned by a 30 minute conditioning cycle at temperature 700°C . Before each test a further pre-test conditioning cycle was carried out at engine speed 1500 rpm. In this cycle, light off was achieved and temperature remained stable for 10 minutes. The catalyst was isolated and the engine was shut down to allow the catalyst to cool down to about 400 K. This temperature was below light off but high enough to avoid the presence of condensed water vapour [17] and the necessity to model it.

The engine was re-started. The thermocouple in the manifold (throat) reached a near stable temperature such that the rate of rise of temperature was less than 1K per 10 seconds. The main valve was opened which diverted the stream through the catalyst. The temperature at inlet to the catalyst was thereby ramped up at a rate of about 5 K/s. The instrumentation was monitored and the run continued until the outlet temperature reached a plateau. The bypass valve was then switched to divert the flow through the bypass. An idle cycle was run for 5 minutes. The test was repeated.

The tests were carried out for engine speeds 1200, 2000 and 3000 rpm. As only one engine bank was used there were four pulses per two engine revolutions. Hence the corresponding mass flow pulsation frequencies were theoretically 40, 67 and 100 Hz, but pressure recordings in the exhaust showed that the dominant frequencies measured were 10, 16 and 25 Hz, probably due to pressure wave effects in the long exhaust duct.

4.0 RESULTS

The engine tests were run for both non-reactive and reactive catalysts, and the results from the former will be discussed first.

4.1 Warm up of non reactive substrates

The main results from the tests for engine speeds 1200 and 2000 rpm are presented here. There was evidence of hydrocarbon conversion at 3000 rpm for washcoated catalysts without precious metal. This is attributable to the washcoat, as the effect is not observed with non-washcoated ceramic substrate. It was therefore not possible to run the CFD model for this condition and perform a valid comparison with experimental temperature measurements. Table 3 lists the experiments that were performed to indicate the range of conditions explored.

Examples of the results are shown in Figures 6 and 7. The bold line is the measured inlet gas temperature. The hashed lines show the CFD predictions of temperature as a function of time at four different positions, the z location being 35, 50, 70 and 85 mm from the inlet face. The symbols in Figs. 6 and 7 denote measured temperatures from thermocouples in the engine tests and these also

correspond to positions 1 to 4. These measurements were recorded to the nearest 5K and this is the explanation for the discontinuous nature of some of the data plots.

Figure 6 shows the results for Tests 121 and 122. Figure 7 shows the results for Tests 133 and 106. Agreement is fair for Test 121 and is good for Test 122. The substrate is warmer than predicted at early times; its temperature appears to respond more quickly to the incoming gas than the CFD model predicts. This is consistent with observations [19] in hot air flow test rig studies.

The CFD model predicts a notable cooling of the substrate in Fig. 7 by the incoming gas at early times, which is not seen in practice. The substrate is therefore again warmer in reality than is predicted for times early in the warm up process. The cooling of the substrate by the incoming gas is predicted to a lesser extent for the other substrates; the 600/4 ceramic is the most responsive sample. Overall agreement between measured and predicted temperatures is fair in Tests 106 and 133.

The case Test 106 at engine speed 2000 rpm, was studied as a simple pulsating flow case. The pulsating mass flow rate was entered into the model as $0.01345 + 0.01076 \sin(2\pi t/T)$ kg/s where period T was 0.0625 secs. There were 40 time steps per cycle so that the time step was 0.0015625 secs. The effect of pulsations on the predicted solid temperatures for the positions monitored in the engine tests can be seen in Fig. 8 to be negligibly small. Thus inclusion of pulsating flow in the simulation did not improve on the degree of agreement seen in Figure 7.

It was found that agreement between predictions and data was generally better at the higher engine speed, i.e. for the higher mass flow rate. Although agreement was not good for all times, in many cases there was fortuitous correspondence in the region of 500 K, the temperature at which light off is initiated.

4.2 Warm up and conversion by reactive substrates

The data obtained from all the experimental engine tests on reactive catalysts are presented here. Figures 9A and 9B show the measured conversion fractions for hydrocarbons for the three engine speeds, 1200, 2000 and 3000 rpm. The 600/4 ceramic sample can be seen to initiate light off most

rapidly (Fig. 9A) and the 800/2 metallic sample least rapidly (Fig. 9B). An indication of the relative response of different substrates to warm up prior to light off is given by the value of parameter $[h A_v / \rho C_p]$ in Table 2, but the respective inlet temperature ramps have a controlling effect in Figures 9A and 9B. Figure 10 shows the gas inlet temperature ramps in the tests at 2000 and 3000 rpm.

Table 4 lists the engine tests carried out on reactive catalysts at the higher two engine speeds, 2000 and 3000 rpm. These tests were compared with CFD predictions. The conditions were fuel rich in every case and so the CFD model included NO reduction by CO, as described above. Fig. 11 shows the hydrocarbon conversion results for Test 118 compared with alternative CFD predictions. The closest agreement can be seen to be achieved by using Cundari and Nuti rate constants together with an arbitrary multiplier, M, of 5. Fig. 12 shows a similar comparison for substrate temperatures. Use of the Cundari and Nuti rate constants can be seen to predict the highest temperatures and the lowest light off temperature, although the temperatures predicted by the different schemes diverge significantly only after initiation of light off. All of the simulations for investigation of onset of light off were run with these values.

Fig. 13 shows a simulation of the pulse shape for one engine bank over 720 degrees (0.04 secs) at 3000 rpm. Forty data points characterise the trace with 19.6 g/s of mean mass flow (cf. 19.8 g/s in test). The CFD model was run for pulsating flow using the values from Figure 13 as input, and was run steady using 19.6 g/s as inlet mass flow. The effect on predicted temperature is seen in Fig. 14 to be very small. In the pulsating flow case the conversion was mass flow rate weighted through the cycle and then cycle averaged. Comparison of conversion in the steady flow case and in the pulsing flow case is seen in Fig. 15 and the effect of pulsating flow on conversion is also seen to be small. Steady flow CFD prediction was therefore used subsequently to make predictions for the test cases with consequent savings in computing time. The effects of pulsating flow per se are not investigated in this paper but have been investigated in earlier work by the authors [**11,18**].

The simulations were therefore run as 1D steady flow thermally transient reactive cases and compared with the results from the engine tests. Figure 16 shows an example of the predicted values for conversion and temperature compared with the data from engine Test 102 at 3000 rpm. Figure 16A

shows a plot of conversion fraction against time and Figure 16B shows the same data but plotted against substrate temperature at $z = 35$ mm. Figure 16C shows measured and predicted substrate temperatures. Solid temperature is reasonably well predicted for the front of the substrate at around the time of light off but there are discrepancies in solid temperature predictions at low and high times. This tendency for the substrate to warm up more rapidly than predicted at low times, but later to lag behind the predictions, was observed in all cases.

Figures 17 and 18 show plots similar to Figures 16A and B for the other engine tests. Figure 17 shows results for the ceramic samples and Figure 18 shows results for the metallic samples. In Figure 17 agreement is slightly better at 2000 rpm (Fig. 17A, B, E and F) than at 3000 rpm (Fig. 17C, D, G and H). Table 4 shows that species concentrations, mass flows and initial temperatures were consistent in the tests with different substrates and engine speeds. Table 2 shows that parameter $[hA_v/(\rho C_p)]$ is high for the 600/4 ceramic, which would imply faster light off, [12], but that its value is also high for the 800/2 metallic sample. The faster light off of the 600/4 sample (Fig. 17G) is due to a more rapid inlet temperature ramp, see Figure 10, in those tests. In Figure 18 the degree of agreement is similar at 2000 and 3000 rpm. The time for 50 % conversion of hydrocarbon is approximated in both the 2000 rpm (13.5 g/s approx.) and 3000 rpm (19.75 g/s approx.) cases in Figure 18. This suggests that the scheme describing the chemical kinetics is predicting conversion as a function of temperature correctly during the early part of the light off. Prediction of temperature itself is still imperfect, as exemplified by the non-reactive warm up studies presented in the first part of this paper and by Figure 16. Predictions of the onset of light off are dependent upon the ability of the model to predict temperature accurately pre light-off. In both Figure 17 and Figure 18 it is apparent that predictions of hydrocarbon conversion levels after light off are not good. This is attributable to the limitations of the chemical scheme used in this study under fuel rich conditions. A more complex chemical scheme would be required to more accurately predict conversion levels post light-off.

The ability of the model, which is based on a simplified reaction scheme, to predict the onset of light off for a range of conditions, namely for different substrates, for different engine operating conditions and for different inlet temperature ramps, has thus been explored. The strengths and limitations of this modeling approach have been demonstrated

5.0 CONCLUSIONS

The results show that model predicts temperature fairly well for some higher flow rate non-reactive cases, but less well for the lower flow rate cases, where the tendency for the substrates to warm up faster than predicted at low times has been observed. In the reactive cases too this same tendency is observed. For the reactive cases, generally, onset of light off is correctly predicted if temperature is correctly predicted. The agreement noted between measurements and predictions is found to be slightly better for the metallic substrates investigated than for the ceramic substrates. The modelling approach for predicting the onset of light off has been demonstrated for a range of practical catalyst substrates.

The level of agreement between measurements and CFD predictions of onset of light off achieved in these studies was obtained by using reaction rate constants based on the Cundari and Nuti [15] scheme. The activation energies are not changed but in order to achieve better agreement the pre-exponential factors are increased. Where agreement between measurements and predictions is less good, the light off occurs even earlier than is predicted by the modified scheme. This is attributed to temperature predictions that are too low in the early stages of warm up. The classic scheme of Oh and Cavendish [1] , based on the work of Voltz et al. [13] , did not predict the reactivity correctly in the cases studied here where the exhaust was fuel rich. It was necessary to use higher reaction rate constants to enable the predictions to match the observed data in the early stages of light off.

Running the CFD model for pulsating mass flow, sinusoidal or based on a simulated engine pulse shape, makes very little difference to the predictions when compared with steady flow predictions. This is true for both temperature and conversion in the cases studied here, where the temperature ramp of the exhaust gas was about 5 K/s. Steady flow predictions therefore seem to be adequate in cases of this type and to offer a considerable saving in computation time when simulating pulsating flow cases.

It is clear that correct prediction of temperature pre light-off is necessary in order to predict the onset of light off. In some instances, even with non-reactive substrates, improvements in the accuracy of temperature prediction should be attainable. Future work could look again at this. The model described

in this paper is a simple approximation to the real situation. The description of the chemical processes is an approximation to a complex scheme. The pre-exponential factors in the reaction rate constants used are adjusted from those in the literature. Previous authors have not used the Cundari and Nuti reaction rate constants for CO in conjunction with the Siemund et al. values for NO. Some of the parameters in the CFD model, such as specific heats and mass transfer coefficients, are held constant at values appropriate for temperatures in the region of the light off temperature. Allowing these to vary with temperature slows down the model and has little influence on light-off predictions. Overall, the simple model provides predictions of the onset of light off that can be computed rapidly and that compare fairly well with real engine test data, but a more complex reaction scheme would be required for prediction of conversion levels post light-off in fuel rich cases.

ACKNOWLEDGEMENTS

The authors acknowledge ArvinMeritor Ltd., Ford Motor Company, Jaguar Cars Ltd., and Johnson Matthey plc; the project was supported under the SERC-DTI Link Programme on Applied Catalysis which funded the research project.

REFERENCES

- [1] **S. E. Oh. J. C. Cavendish.** Transients of monolithic catalytic converters: Response to step changes in feedstream temperature as related to controlling automobile emissions. *Ind Eng Chem Prod Res Dev* 21 (1982) pp 29 - 37

- [2] **N. Fueyo.** 1D simulation of a catalytic converter for cars. *Phoenix demonstration Report* PDR/CFDU/IC/35, CHAM Ltd. (1987)

- [3] **S. Tagliaferri. L. Padeste. A. Baiker.** Behaviour of three way catalysts in a hybrid drive system: dynamic measurements and kinetic modelling. *Catalysis and Automotive Pollution Control III; Studies in surface science and catalysis* Vol.96 (1995, Elsevier Science) pp 897 - 908

- [4] **S. Siemund. J. P. Leclerc. D. Schweich. M. Prigent. F. Castagna.** Three-way monolithic converter: simulations versus experiments. *Chem Eng Science* Vol 51 (1996) pp 3709 – 3720
- [5] **G. C. Koltsakis. I. P. Kandyas. A. M. Stamatelos.** Three-way catalytic converter modelling and applications. *Chem Eng Comm* Vol. 164 (1998) pp 153 – 189
- [6] **K. N. Pattas. A. M. Stamatelos. P. K. Pistikopoulos. G. C. Koltsakis. P. A. Konstantinidis. E. Volpi. E. Leveroni.** Transient modelling of 3 way catalytic converters. *SAE Paper* 940934 (1994) pp 565 – 578
- [7] **D. Schweich.** Laboratory data for three way catalytic converter modelling. *Catalysis and Automotive Pollution Control III; Studies in surface science and catalysis* Vol.96 (1995, Elsevier Science) pp 55 – 71
- [8] **N. Baba. K. Yokota. S. Matsunaga. S. Kojima. K. Ohsawa. T. Ito. H. Domyo.** Numerical simulation of deactivation process of three way catalytic converters. *SAE Paper* 2000-01-0214 (2000) pp 117 – 132
- [9] **G. McCullough. R. Douglas. G. Cunningham. L. Foley.** The development of a two-dimensional transient catalyst model for direct injection two-stroke applications. *Proc Instn Mech Engrs Vol 215 Part D* Vol 215 (2001) pp 919 - 933
- [10] **F. Lacin. M. Zhuang.** Modeling and simulation of transient thermal and conversion characteristics for catalytic converters. *SAE Paper* 2000-01-0209 (2000) pp 53 - 63
- [11] **S. F. Benjamin. C. A. Roberts.** Warming automotive catalysts with pulsating flows. *Proc Instn Mech Engrs Part D* Vol 215 (2001) pp 891 – 910
- [12] **S. F. Benjamin. C. A. Roberts.** Modelling warm up of an automotive catalyst substrate using the equivalent continuum approach. *Int J Vehicle Design* Vol. 21 (1999) pp 253 – 273

- [13] **S. E. Voltz, C. R. Morgan, D. Liederman, S. M. Jacob.** Kinetic study of carbon monoxide and propylene oxidation on platinum catalysts. *Ind Eng Chem Prod Res Dev* Vol 12 (1973) pp 294 – 301
- [14] **D. K. S. Chen, C. E. Cole.** Numerical simulation and experimental verification of conversion and thermal responses for a Pt/Rh metal monolithic converter. *SAE paper* 890798 (1989) pp 1 – 12
- [15] **D. Cundari, M. Nuti.** A one-dimensional model for monolithic converter: numerical simulation and experimental verification of conversion and thermal responses for two-stroke engine. *SAE Paper* 910668 (1991) pp 45 – 52
- [16] **Chan, S. H., Hoang, D. L., Zhou, P. L.** Heat transfer and chemical kinetics in the exhaust system of a cold start engine fitted with a three-way catalytic converter. *Proc Instn Mech Engrs Part D* (2001) Vol 214 pp 765 - 777
- [17] **Clarkson, R. J., Benjamin, S. F.** Modelling the effect of moisture on catalyst warm up. Paper C496/002/95 *Proceedings of VTMS-2 Conference*, London (1995) pp 555 – 562
- [18] **Benjamin, S. F., Roberts, C. A.** Warm up of an automotive catalyst substrate by pulsating flow: a single channel modeling approach. *Int J Heat and Fluid Flow* (2000) Vol 21 pp 717 – 726
- [19] **Benjamin, S. F., Roberts, C. A.** Warm up of automotive catalyst substrates: comparison of measurements with predictions. *Int Comm Heat Mass Transfer* (1998) Vol 25 pp 19 – 32

Tables

Table 1 Frequency factors and activation energies

| Author | k_{CO} | E_{CO}/R | k_{HC} | E_{HC}/R |
|-------------------------|-----------|------------|-----------|------------|
| Oh and Cavendish [1] | 6.699E+13 | 12556 | 1.392E+15 | 14556 |
| Cundari and Nuti [15] | 6.0E+09 | 6500 | 2.0E+10 | 7100 |
| Koltsakis et al. [5] | 2E+13 | 11427 | 3.0E+14 | 12629 |
| Chan et al. [16] | 1.005E+14 | 16574 | 1.392E+15 | 19250 |

Table 2 Relative properties of washcoated substrates

| Property | 400/6.5 Ceramic | 600/4 Ceramic | 400/2 Metallic | 800/2 Metallic |
|---------------------------------------|---------------------|-----------------|----------------|----------------|
| Wall thickness | 6.5 thou; 0.1651 mm | 4 thou; 0.11 mm | 0.05 mm | 0.03 mm |
| Porosity % | 67.1 | 68.8 | 77.97 | 79.57 |
| Bulk density ρ kg/m ³ | 563 | 533 | 918 | 802 |
| Sp Heat Cp J/(kgK) | 914 | 914 | 567 | 578 |
| Av m ² /m ³ | 2579 | 3199 | 3140 | 4270 |
| Dh mm | 1.04 | 0.86 | 0.995 | 0.744 |
| k [axial] W/(mK) | 0.36 | 0.30 | 1.4 | 1.2 |
| Permeability coeff α | 0.0001 | 0.0001 | 18.95 | 18.2 |
| Permeability coeff β | 714 | 1018 | 460 | 805 |
| Nu No. | 3.608 | 3.608 | 2.4 | 2.7 |
| Parameter [h $Av/(\rho Cp)$] | 0.46 | 0.72 | 0.38 | 0.88 |

Table 3 Non reactive studies

| Test No. | Substrate | Cells | Initial temp T (K) | Speed Rpm | Fuel (kg/hr) | Air/Fuel Ratio | Mass Flow (g/s) Half Engine |
|---------------------|------------------|----------------|-------------------------------|----------------------|-------------------------|---------------------------|--|
| 121 | Ceramic | 400/6.5 Non wc | 390.5 | 1200 | 3.78 | 14.42 | 8.096 |
| 122 | Ceramic | 400/6.5 Non wc | 388 | 2000 | 6.3 | 14.36 | 13.44 |
| 125 | Ceramic | 400/6.5 Wc | 391.75 | 1200 | 3.86 | 14.43 | 8.25 |
| 126 | Ceramic | 400/6.5 Wc | 388 | 2000 | 6.58 | 14.39 | 14.065 |
| 133 | Ceramic | 600/4 Wc | 394.25 | 1200 | 3.82 | 14.44 | 8.19 |
| 106 | Ceramic | 600/4 Wc | 389.25 | 2000 | 6.31 | 14.35 | 13.45 |
| 80 | Metallic | 400/2 Wc | 388 | 1200 | 3.78 | 14.43 | 8.1 |
| 82 | Metallic | 400/2 Wc | 393 | 2000 | 6.27 | 14.35 | 13.37 |
| 130 | Metallic | 800/2 Wc | 390.5 | 1200 | 3.87 | 14.42 | 8.29 |
| 94 | Metallic | 800/2 Wc | 398 | 2000 | 6.45 | 14.35 | 13.75 |

Table 4 Parameter values for reactive simulations

| Test Nos. | Temp | Substrate | Init | Speed | Mass | CO | O2 | C3H6 | NOx |
|-----------|---------------|-----------|-------|-------|--------|---------|---------|---------|----------|
| | ramp | | T | Rpm | Flow | Mass | Mass | Mass | Mass |
| | at inlet | | (K) | | g/s | Frac | Frac | Frac | Frac |
| 117 & 118 | Test 118 | 400/6.5 | 394 | 2000 | 13.45 | 0.00492 | 0.00430 | 0.00196 | 0.000481 |
| | | ceramic | | | | | | | |
| 119 & 120 | Test 120 | 400/6.5 | 395.5 | 3000 | 19.74 | 0.00575 | 0.00449 | 0.00185 | 0.00145 |
| | | ceramic | | | | | | | |
| 111 & 112 | Test 111 | 600/4 | 390 | 2000 | 13.55 | 0.00498 | 0.00466 | 0.00188 | 0.000479 |
| | | ceramic | | | | | | | |
| 113 & 114 | Test 113 | 600/4 | 403 | 3000 | 19.7 | 0.00570 | 0.00484 | 0.00174 | 0.00164 |
| | | ceramic | | | | | | | |
| 87 & 88 | Test 88 | 400/2 | 391 | 2000 | 13.5 | 0.00498 | 0.00466 | 0.00189 | 0.000479 |
| | | metallic | | | | | | | |
| 128 & 129 | Average of | 400/2 | 397 | 3000 | 19.405 | 0.0058 | 0.00505 | 0.00203 | 0.00195 |
| | Tests 128/129 | metallic | | | | | | | |
| 99 & 100 | Average of | 800/2 | 392 | 2000 | 13.66 | 0.00498 | 0.00466 | 0.00189 | 0.000479 |
| | Tests 99/100 | metallic | | | | | | | |
| 101 | Test 101 | 800/2 | 398 | 3000 | 19.8 | 0.00609 | 0.00486 | 0.00192 | 0.00147 |
| | | metallic | | | | | | | |
| 102 | Test 102 | 800/2 | 389 | 3000 | 19.8 | 0.00609 | 0.00486 | 0.00192 | 0.00147 |
| | | metallic | | | | | | | |

Captions for Figures

(1) Reaction rate constants.

(2) Predicted CO and hydrocarbon concentration through light off at exit from 70 mm length channel.

Legend shows kinetic rate constant multiplier M, mass flow rate in g/s and species.

(3) Comparison of predicted conversion curves for [A] CO and [B] HC, hydrocarbon, at Z 69 mm from inlet, for steady and pulsing conditions. MWCA indicates mass flow-weighted cycle-averaged values, as equation (22).

(4) Predicted concentration at exit through a cycle of mass flow pulsation. Iter denotes the time step in the CFD simulation.

(5) Schematic diagram of engine test rig

(6) Warm up of non-washcoated 400 cpsi ceramic sample. T/C indicates thermocouple measurement.

(7) Warm up of washcoated non-reactive 600 cpsi ceramic sample. T/C indicates thermocouple measurement.

(8) Comparison of CFD predictions for steady and pulsing mass flows

(9A) Conversion observed in engine tests on two different ceramic samples at 1200, 2000 and 3000 rpm

(9B) Conversion observed in engine tests on two different metallic samples at 1200, 2000 and 3000 rpm

(10) Gas inlet temperature ramps in engine tests of reactive samples

(11) Hydrocarbon conversion data from Engine Test 118 compared with CFD predictions using alternative kinetic schemes. C&N indicates Cundari and Nuti,[15]; Oh & C indicates Oh and Cavendish [1].

(12) Temperature data from Engine Test 118 compared with CFD predictions using alternative chemical schemes. C&N indicates Cundari and Nuti,[15]; Oh & C indicates Oh and Cavendish [1]. T/C indicates thermocouple measurement.

(13) Simulated pulse shape from one engine bank

(14) Effect of pulsations on predicted temperatures

(15) Effect of pulsations on predicted conversion

(16) CFD predictions compared with data for Test 102 at 3000 rpm

(17) Predicted conversion compared with data for ceramic samples; T K is solid temperature at Z 35 mm

(18) Predicted conversion compared with data for metallic samples; T K is solid temperature at Z 35 mm

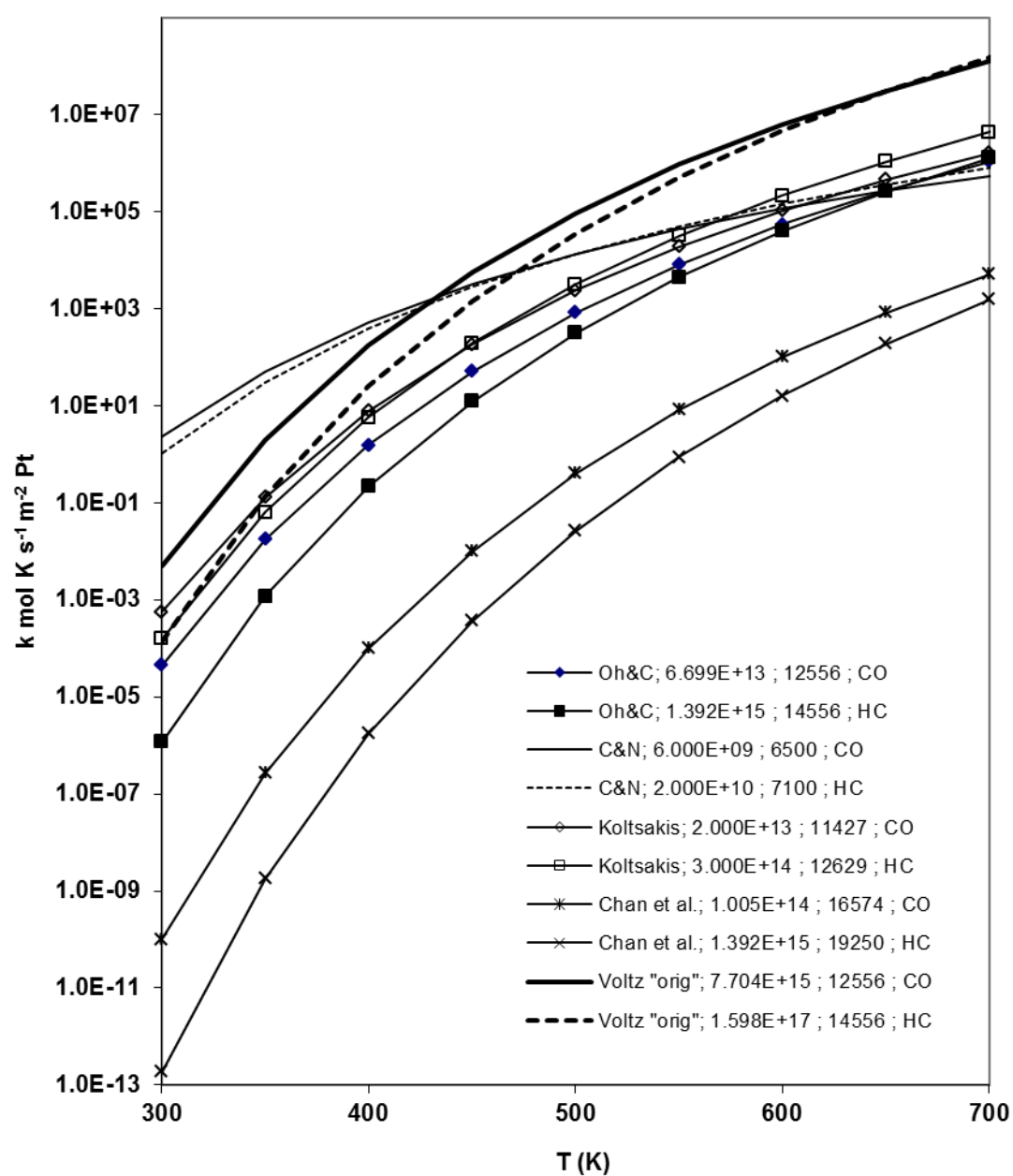


Figure 1

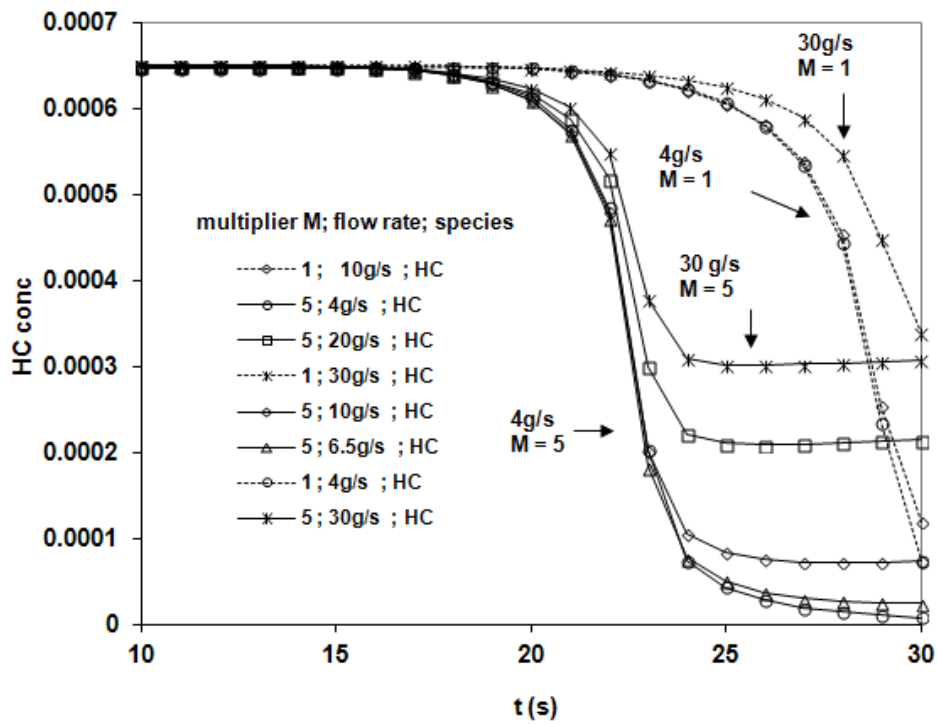
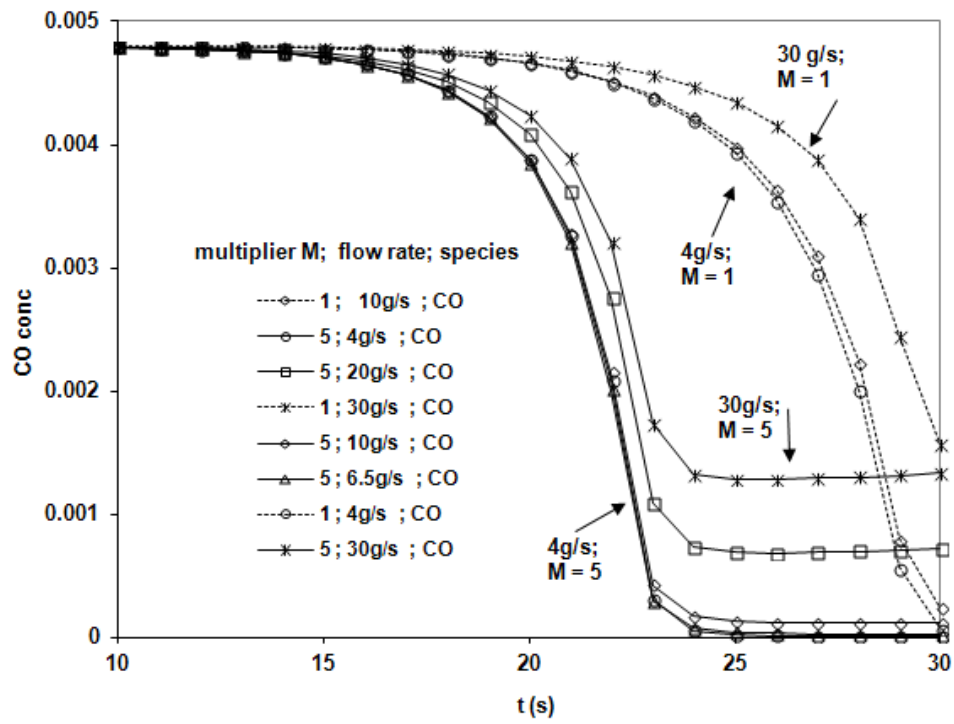


Figure 2

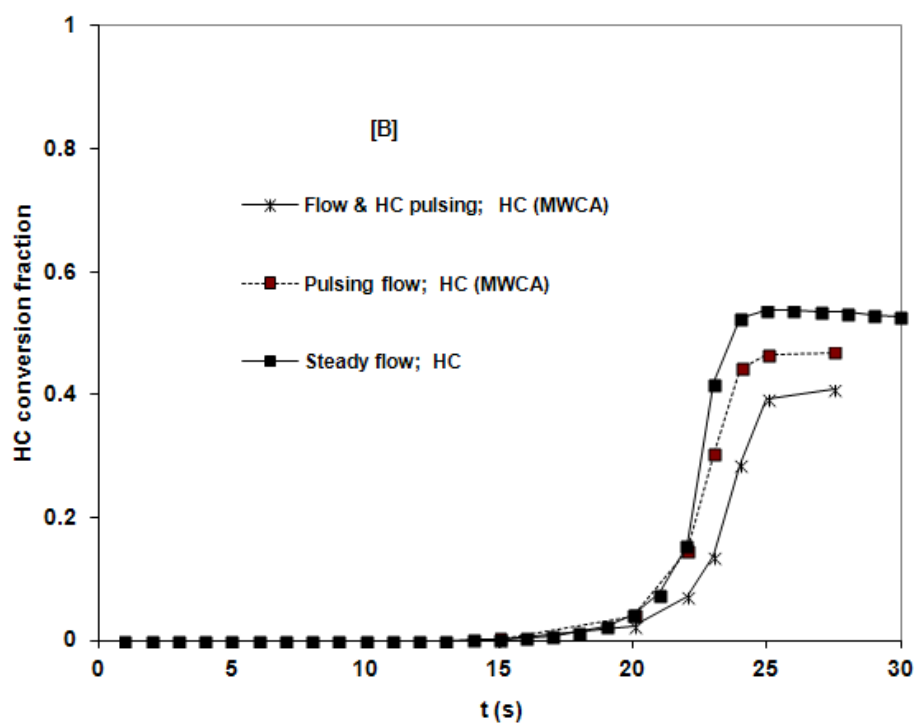
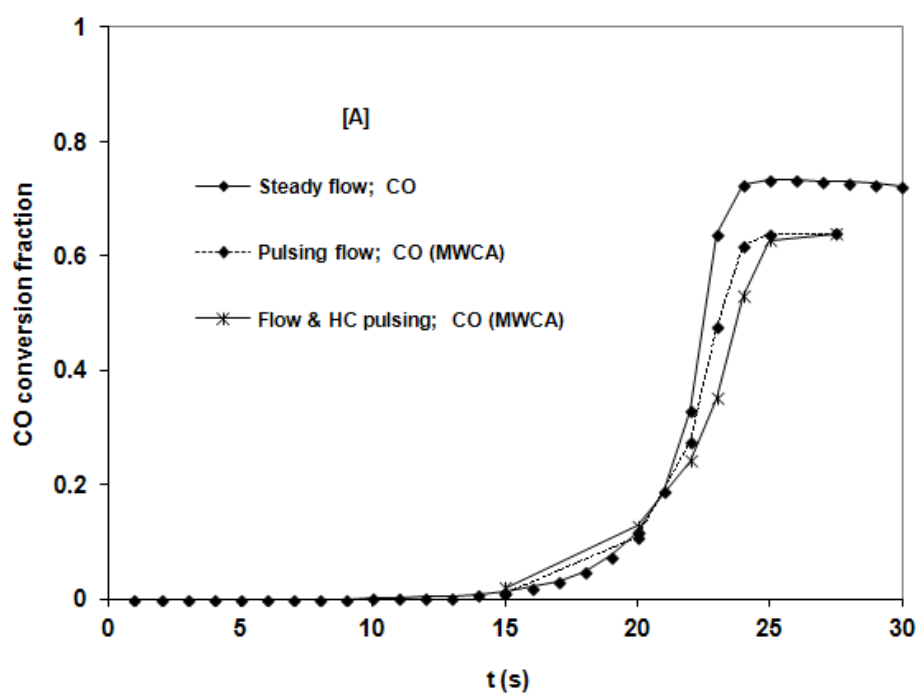


Figure 3

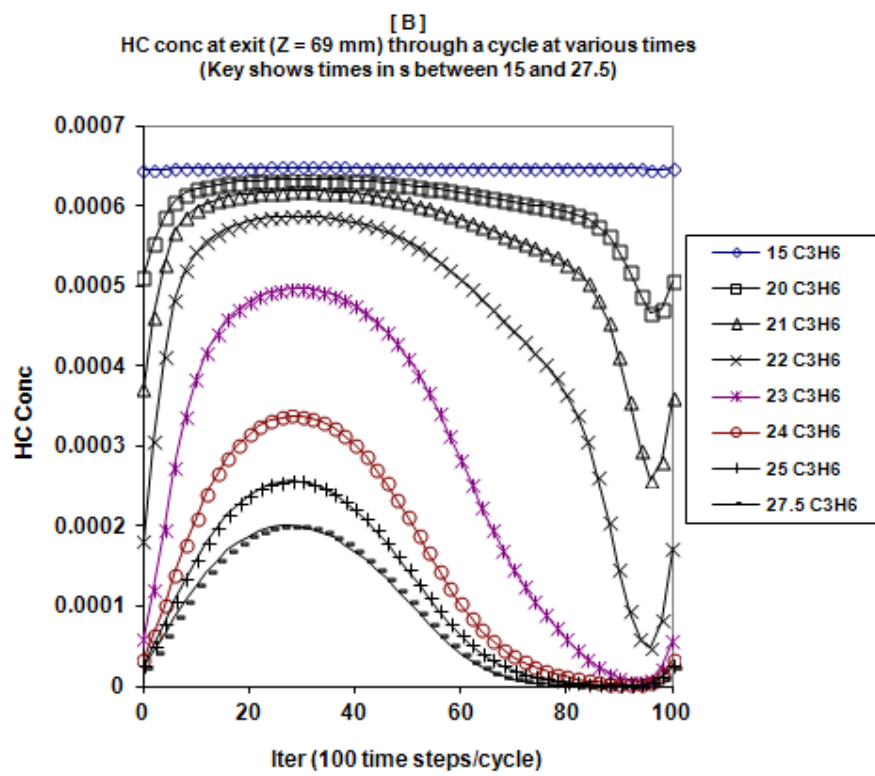
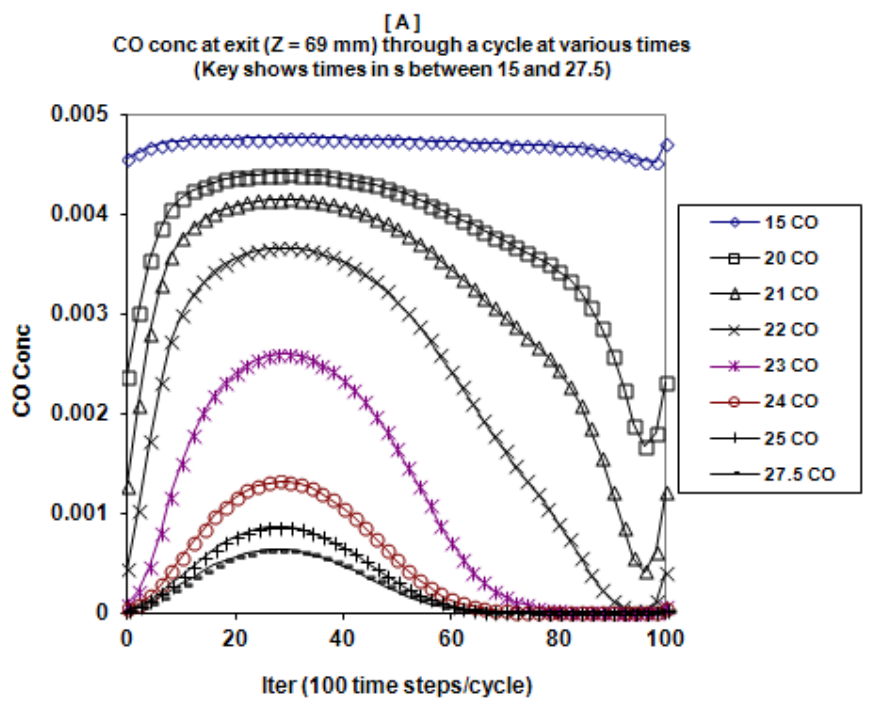


Figure 4

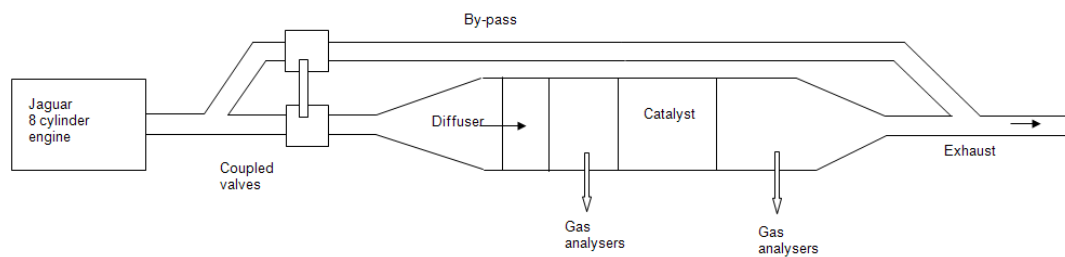


Figure 5

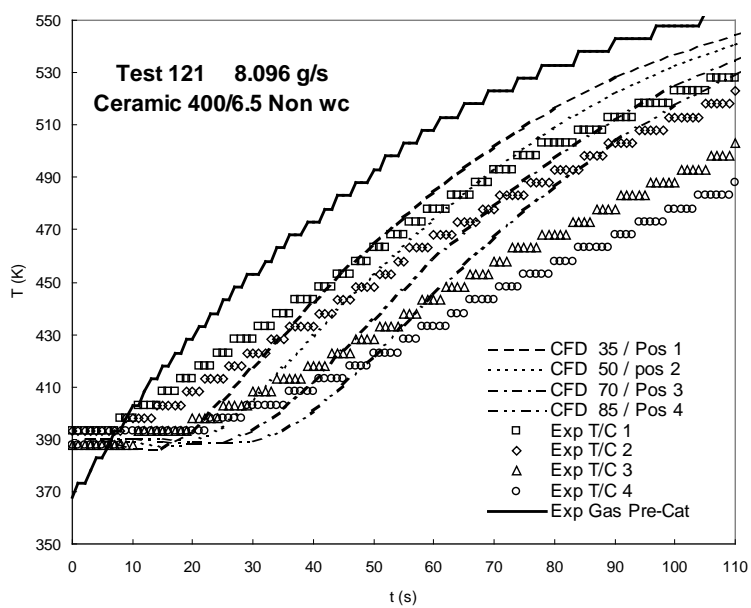
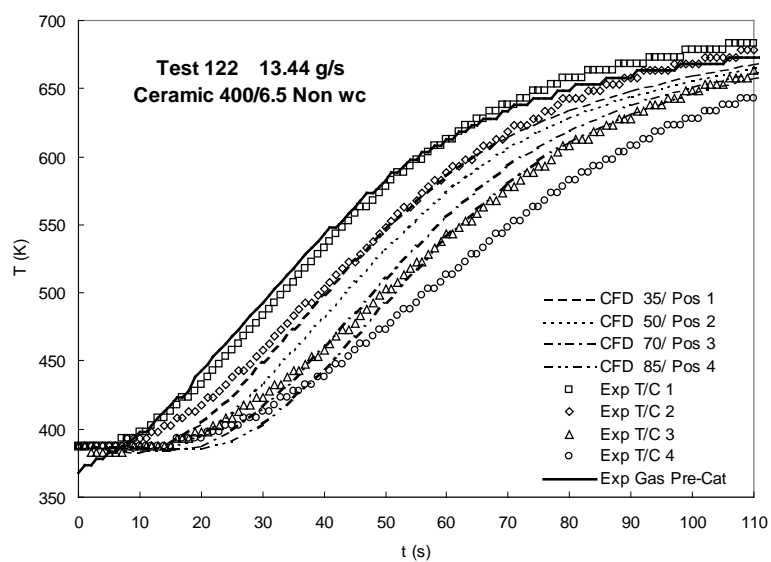


Figure 6

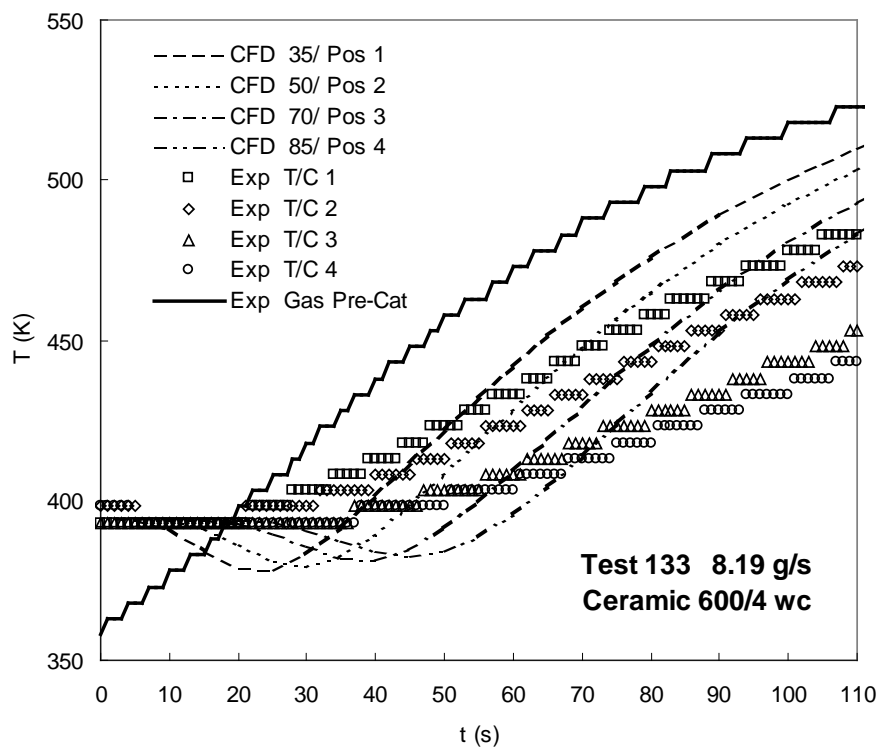
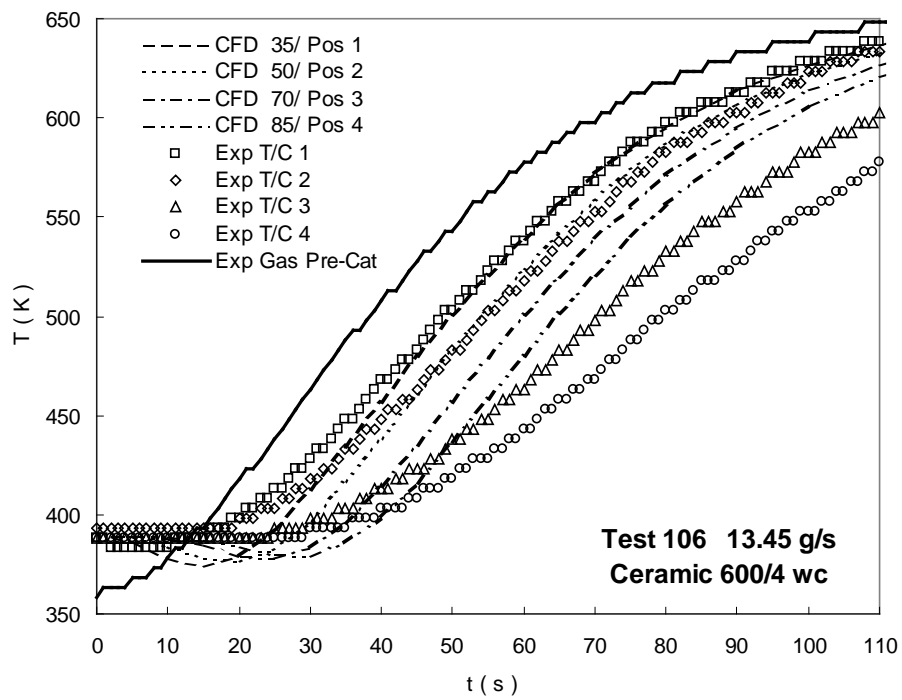


Figure 7

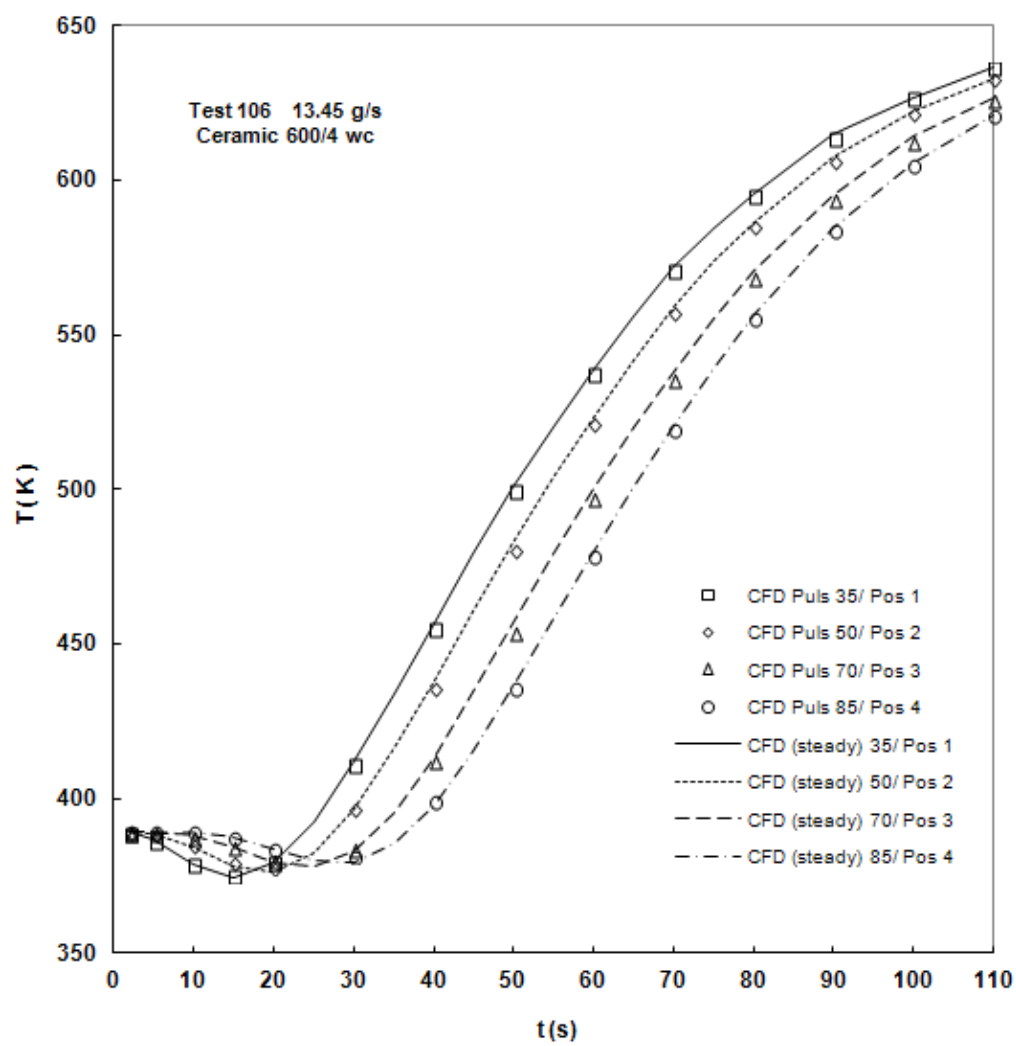


Figure 8

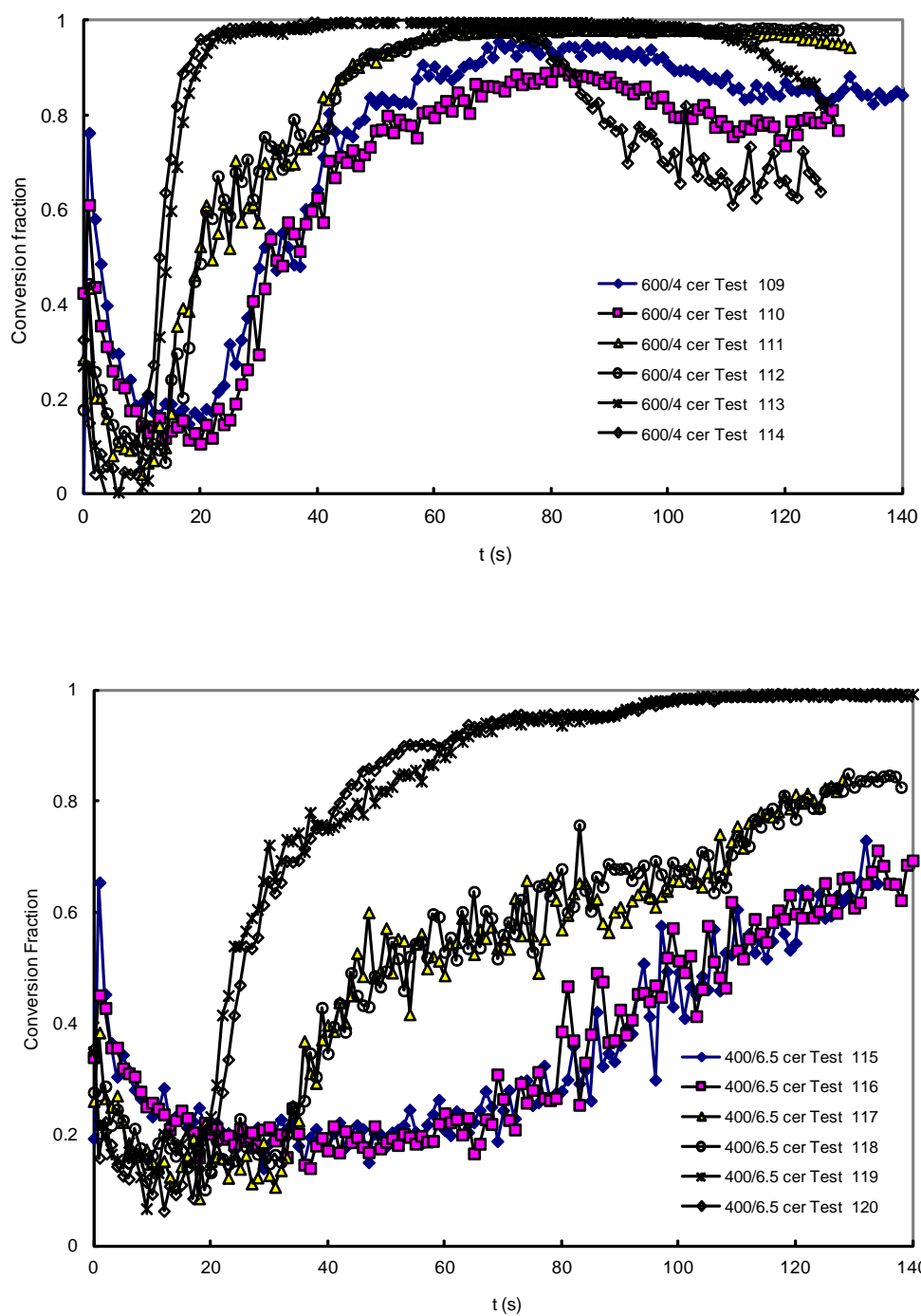


Figure 9A

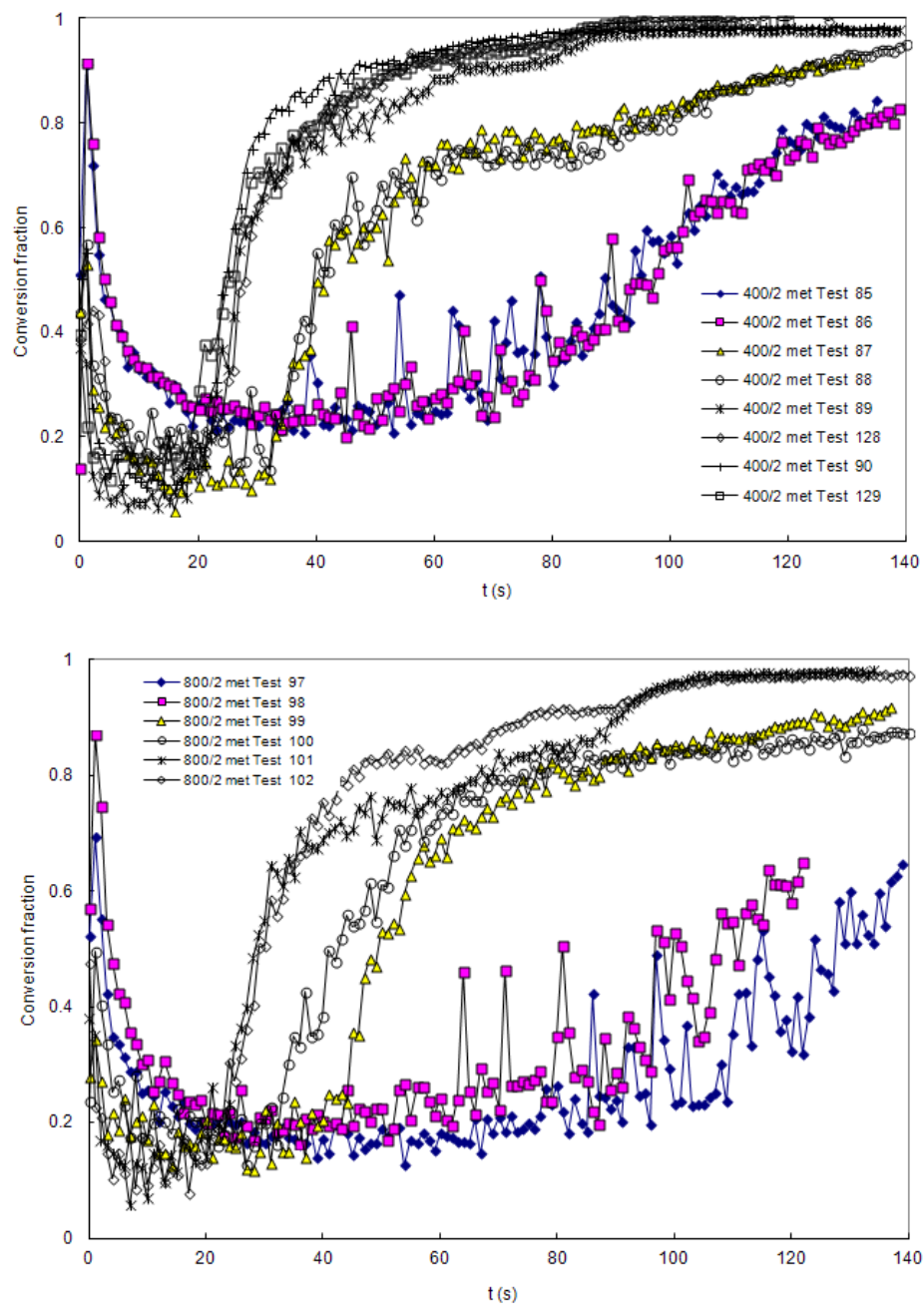


Figure 9B

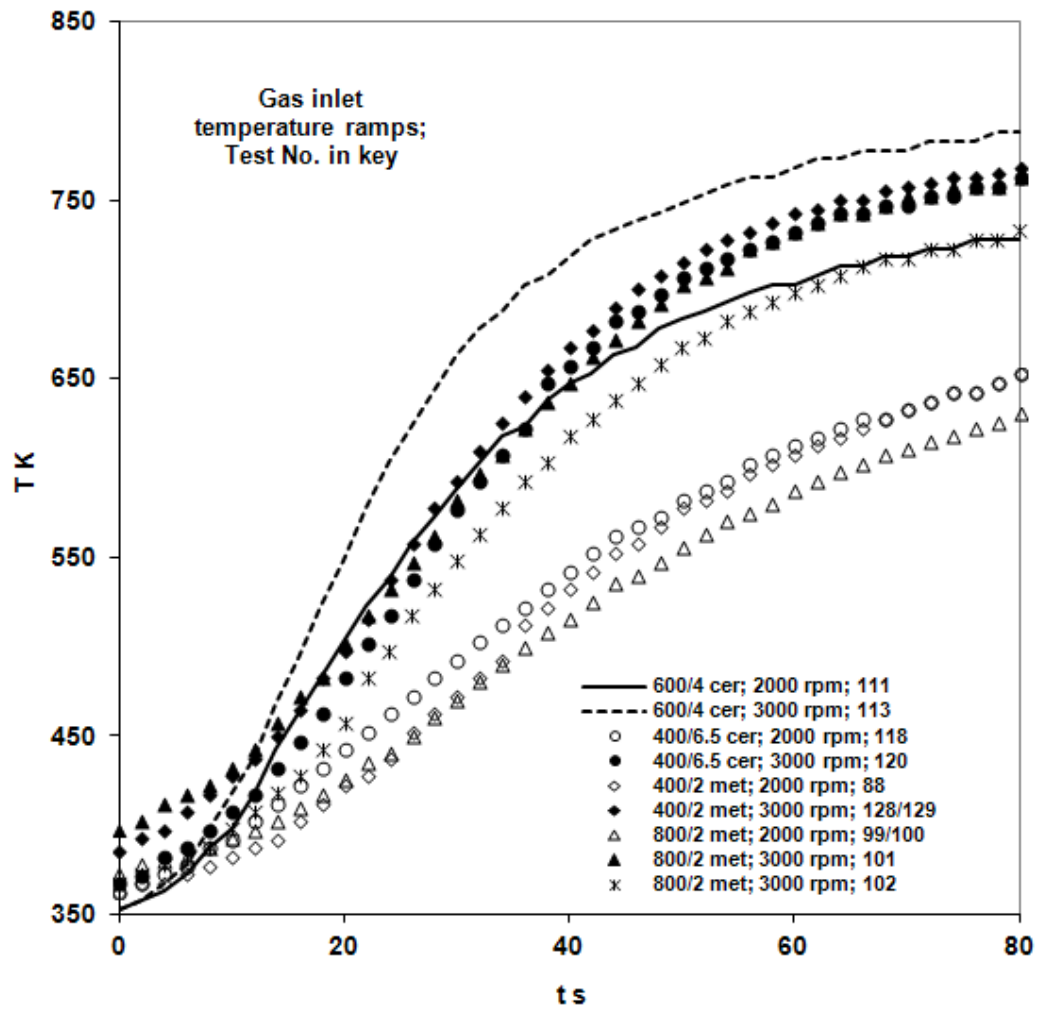


Figure 10

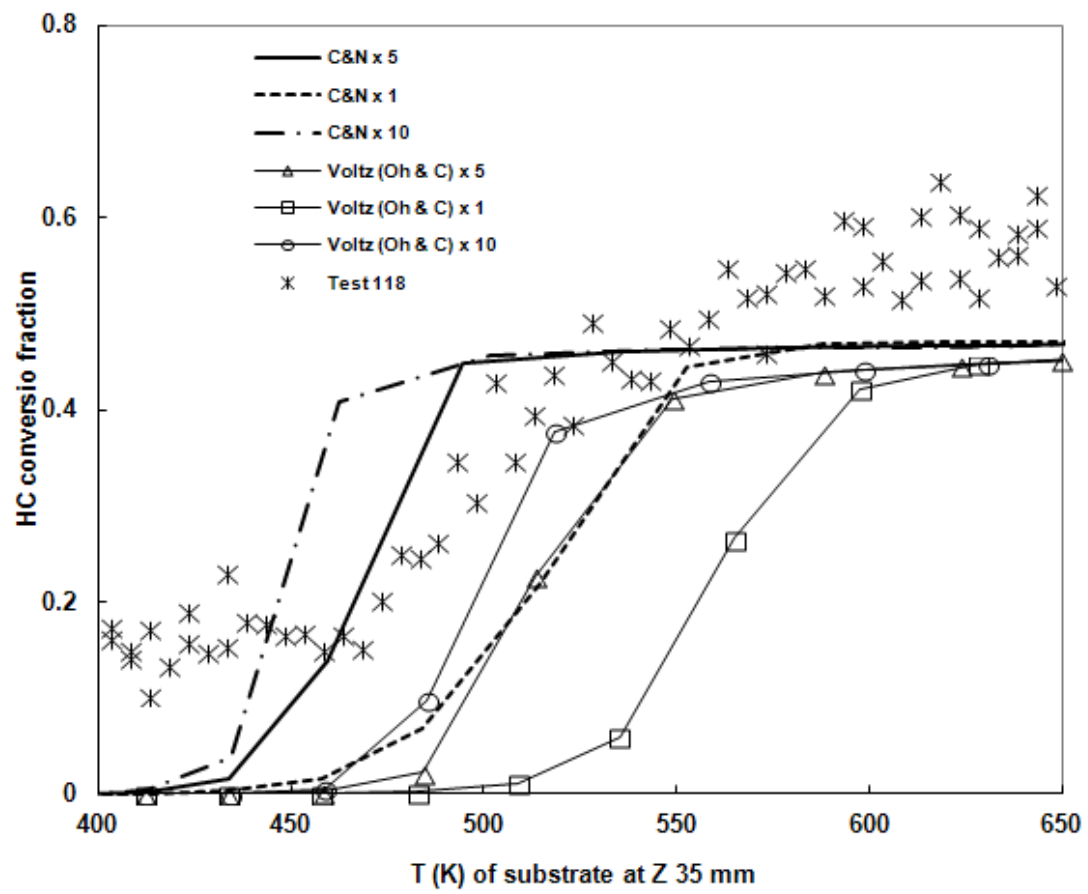


Figure 11

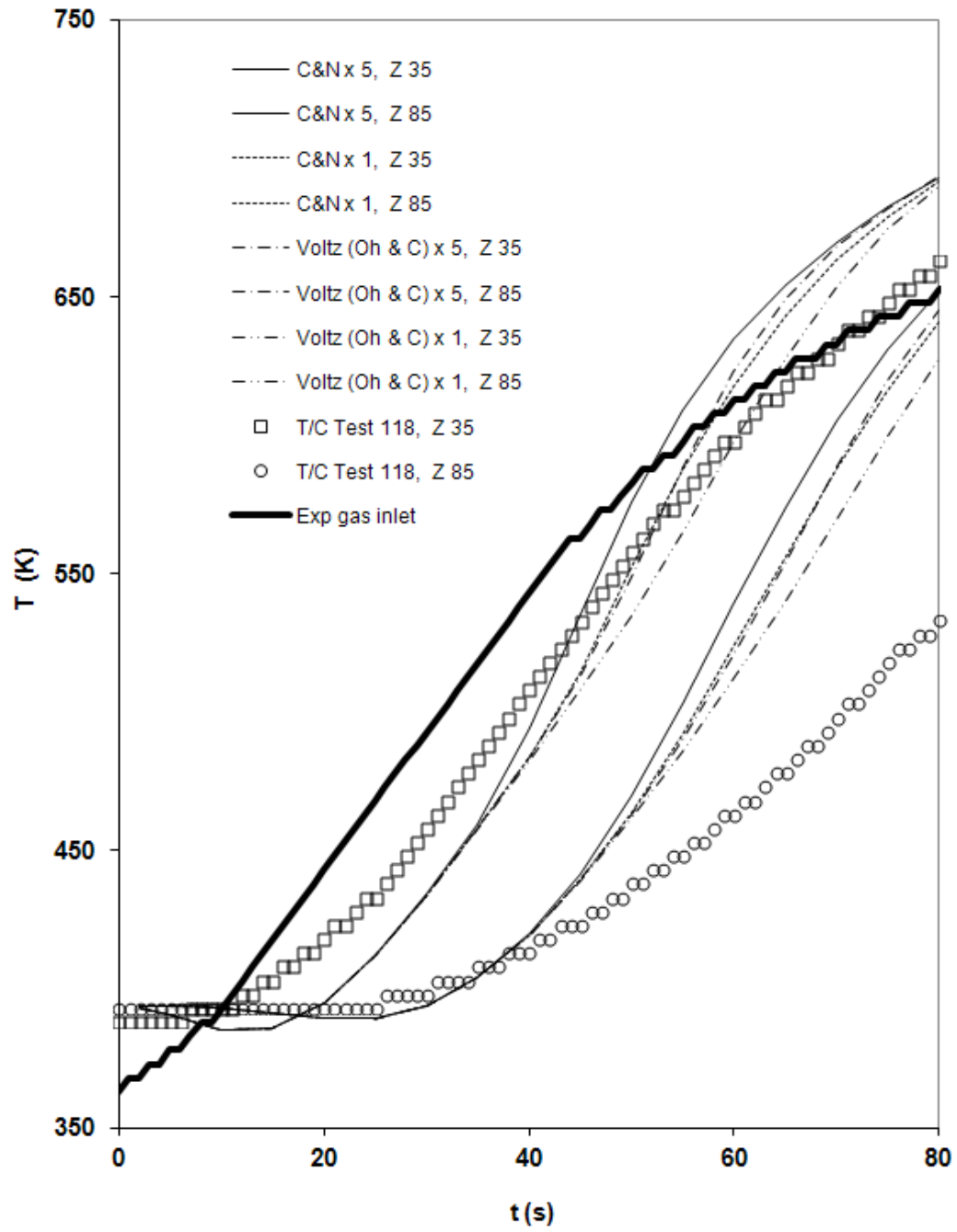


Figure 12

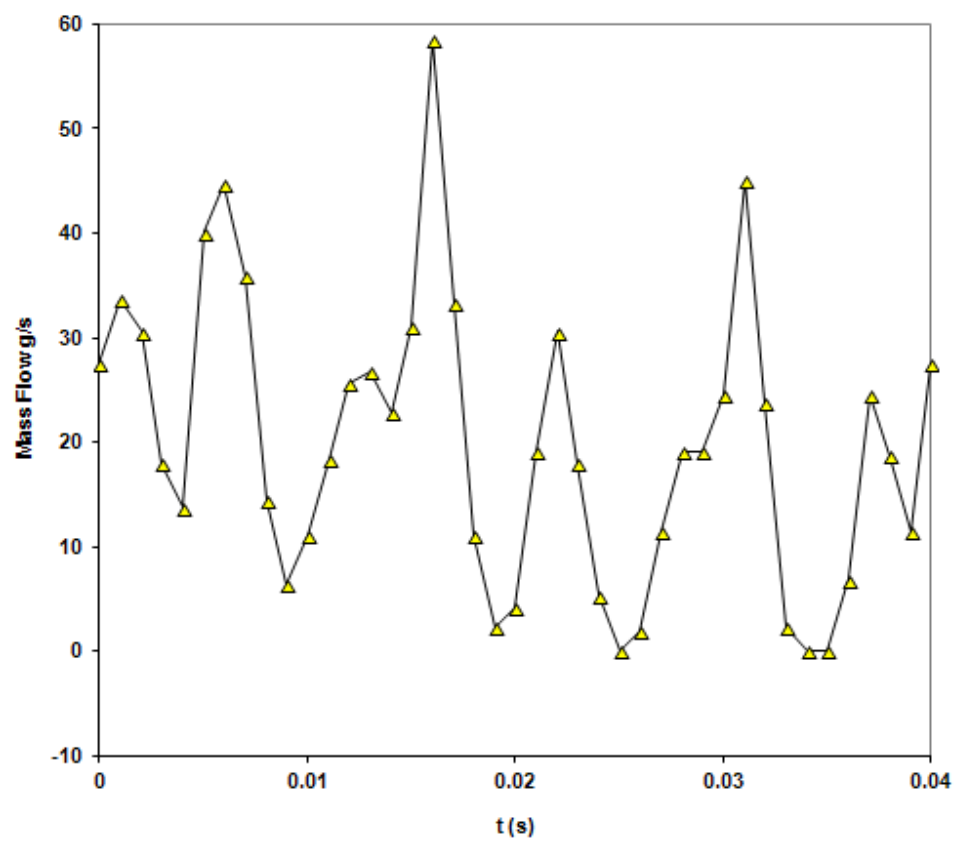


Figure 13

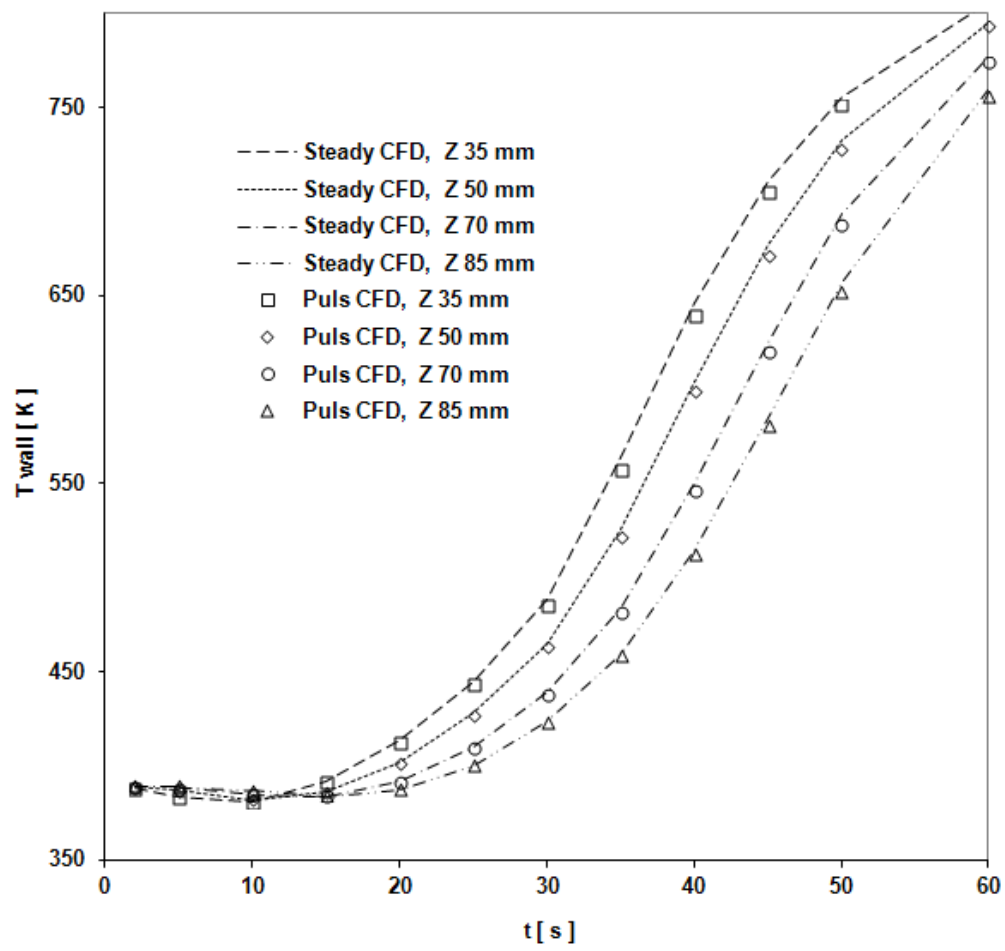


Figure 14

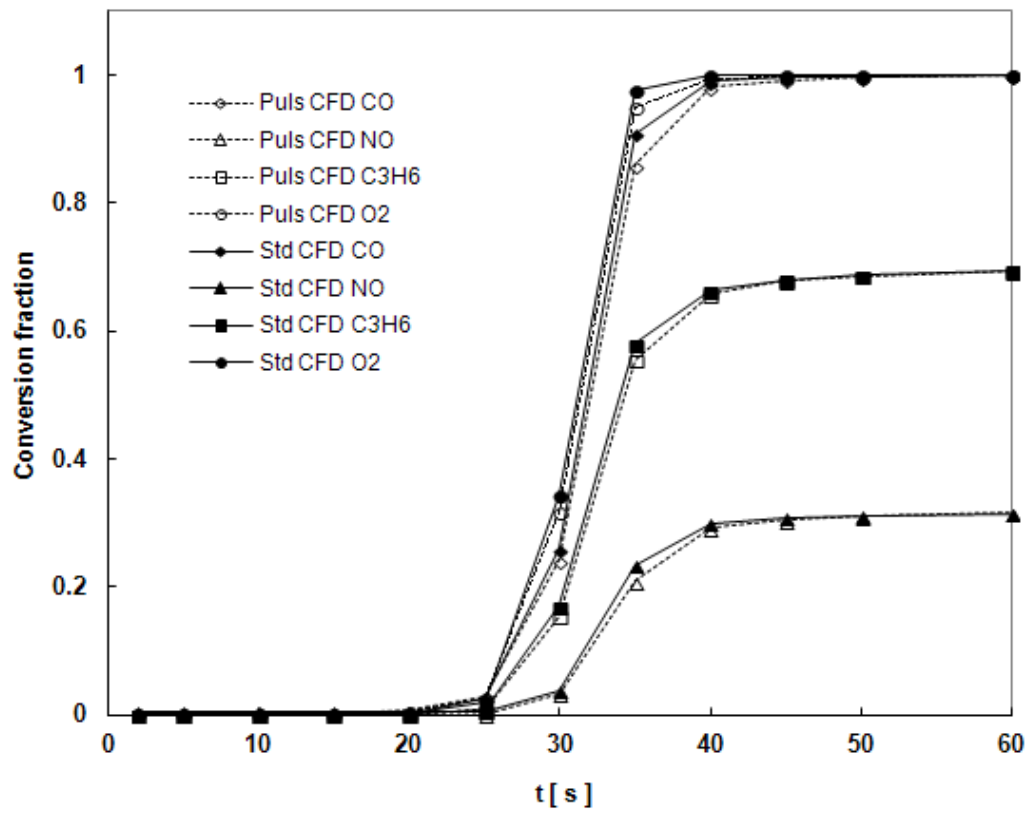


Figure 15

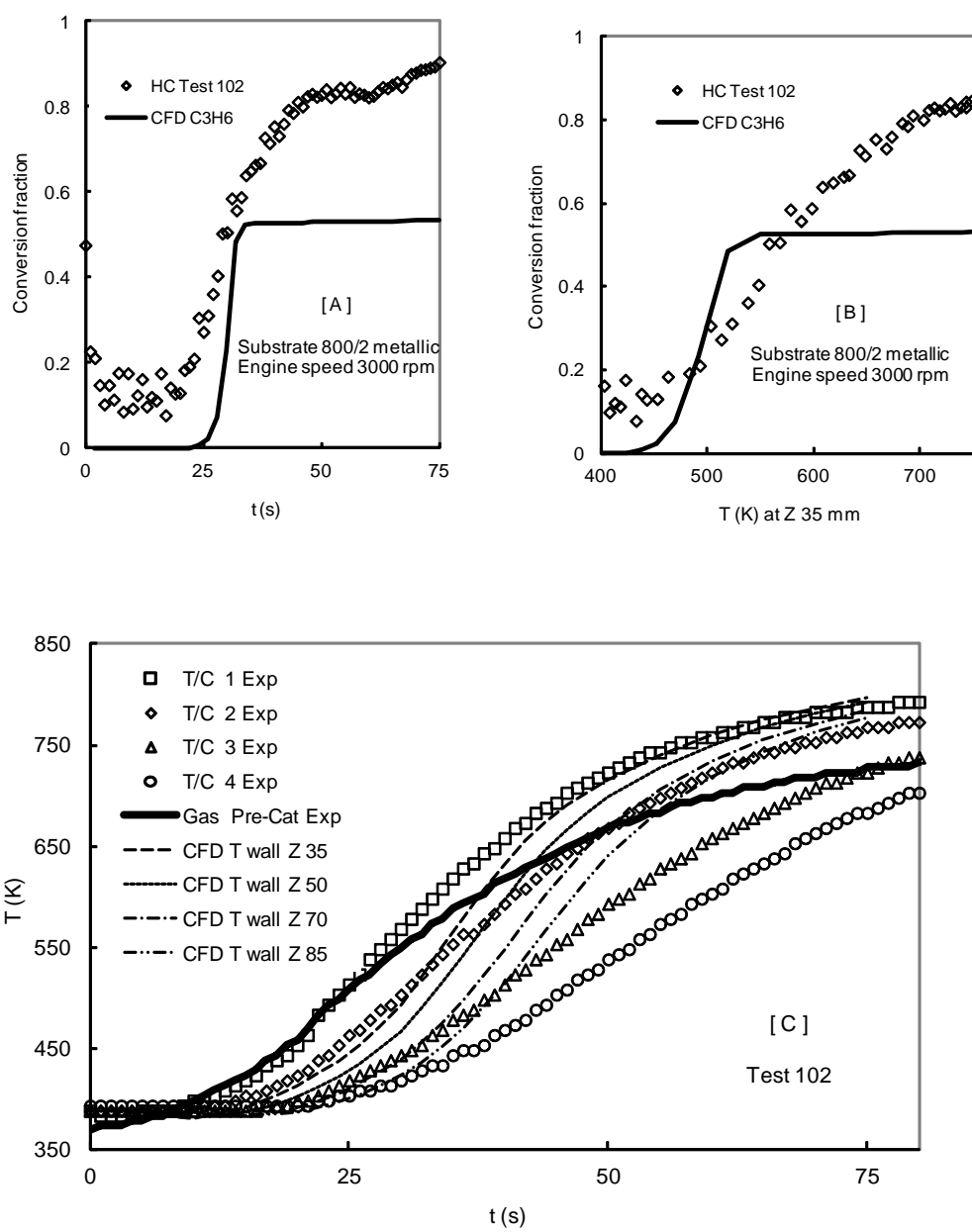


Figure 16

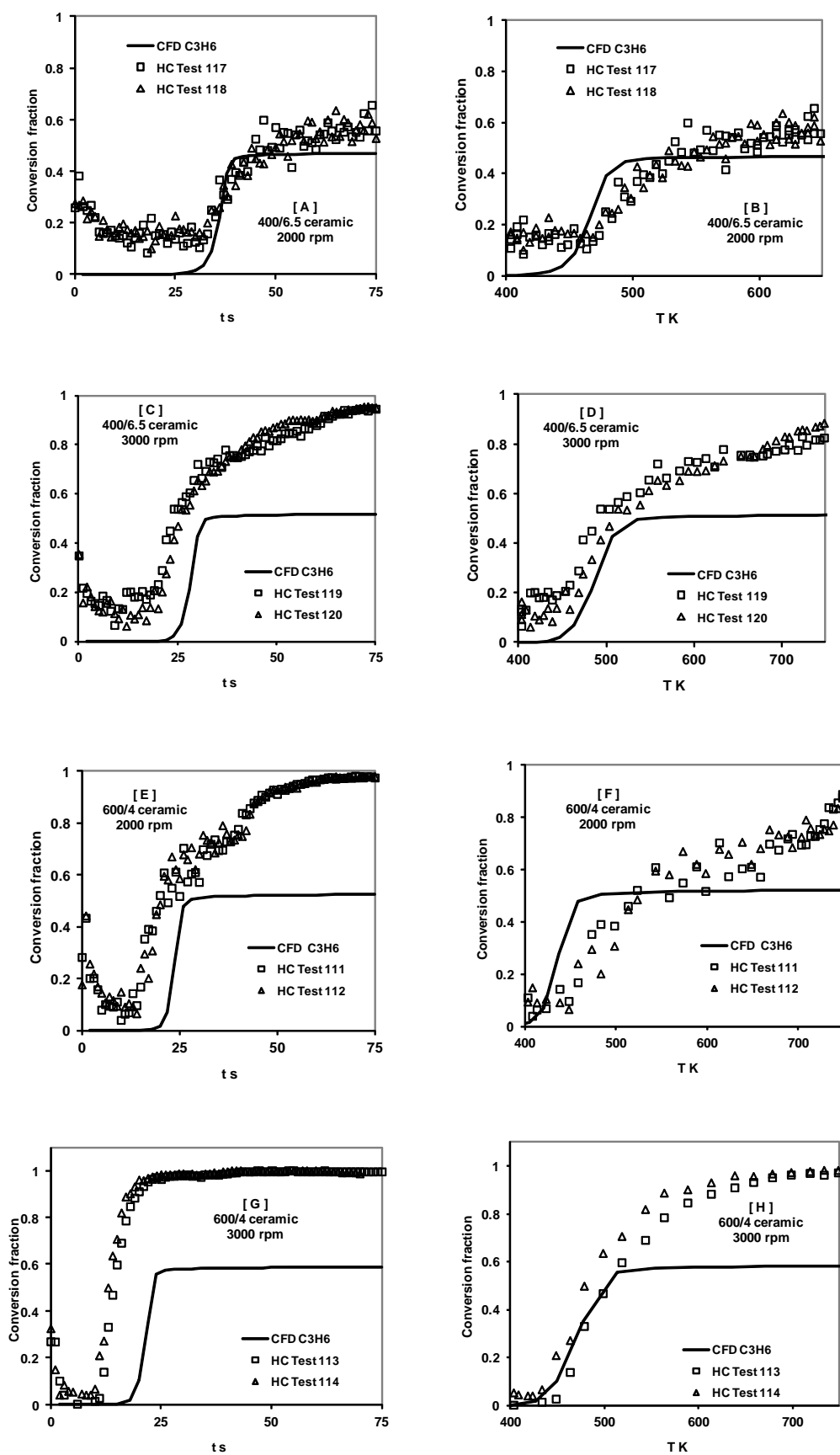


Figure 17

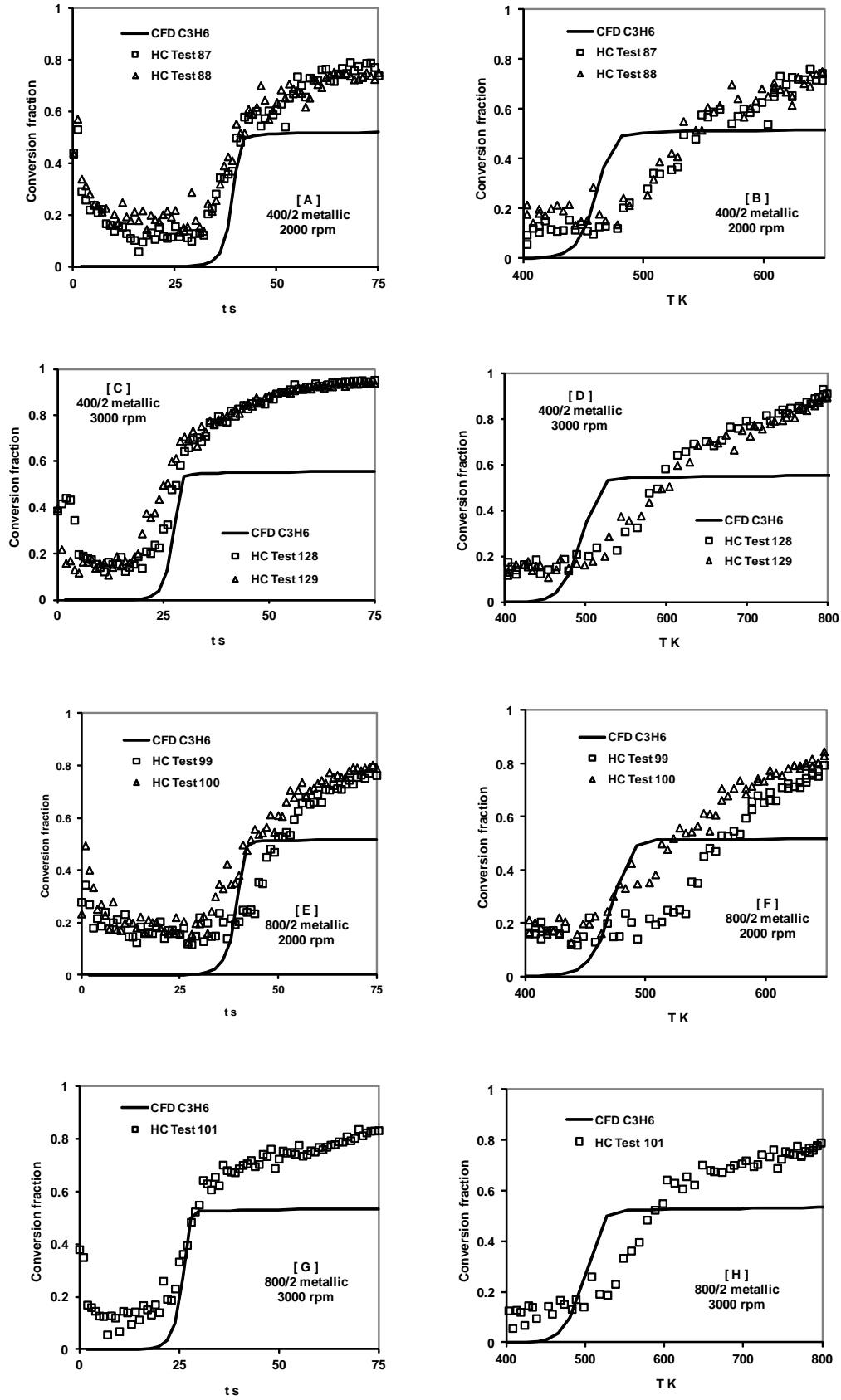


Figure 18

